JOURNAL OF GEOPHYSICAL RESEARCH, VOL. 92, NO. B9, PAGES 9193–9213, AUGUST 10, 1987

Role of Asthenosphere and Lithosphere in the Genesis of Late Cenozoic Basaltic Rocks From the Rio Grande Rift and Adjacent Regions of the Southwestern United States

FRANK V. PERRY

Isotope and Nuclear Chemistry Division, Los Alamos National Laboratory, Los Alamos, New Mexico

W. SCOTT BALDRIDGE

Earth and Space Sciences Division, Los Alamos National Laboratory, Los Alamos, New Mexico

DONALD J. DEPAOLO

Department of Earth and Space Sciences, University of California, Los Angeles

Late Cenozoic alkalic and tholeiitic basalts from the Rio Grande rift region display a wide range of Nd and Sr isotopic compositions which indicate the involvement of "enriched" mantle (EM), "depleted" mantle (DM), and crust in basalt petrogenesis. Isotopic compositions of alkali basalts (this study and published data) reflect the characteristics of their mantle source and correlate with tectonic setting: In the southern Basin and Range, a region of pronounced lithospheric extension and thinning, alkali basalts with $\varepsilon_{Nd} = +7$ to $+8$ are derived from DM, which corresponds to upwelled, oceanic-type asthenosphere; alkali basalts from the Great Plains, northern Rio Grande rift, and eastern Colorado Plateau, regions which have undergone less lithospheric extension, have distinctly different isotopic compositions ($\varepsilon_{Nd} = 0$ to $+2$) and were derived from EM; alkali basalts from the southeastern Colorado Plateau–Basin and Range transition zone have isotopic compositions that are intermediate between DM and EM values ($\varepsilon_{Nd} = +6.6$ to $+3.3$) and were derived from the DM/EM boundary. The correlation of isotopic signatures and upper mantle geophysical properties with tectonic setting suggests a physical model for the evolution of basalt sources during lithospheric extension and rifting. Prior to regional extension and rifting, EM corresponds to lithospheric mantle with a history of trace element enrichment and isolation from the underlying asthenosphere. Once rifting begins, lithospheric extension and asthenospheric upwelling lead to thermal thinning and conversion of lithospheric mantle to asthenosphere. EM can take on asthenospheric physical properties, yet remain intact and a source of basalts until, at an advanced stage of rifting, it is physically replaced by convective mixing with the underlying DM/asthenosphere. Tholeiites, because they equilibrate at shallower depths than alkali basalts, generally equilibrate within EM. In contrast to alkali basalts, tholeiites typically are crustally contamined, probably because their lower volatile contents inhibit their ascent through the crust. Throughout much of the region, tholeiites assimilated small amounts (<10%) of middle to upper crustal wall rock. In contrast, a variety of volcanic rocks (including tholeiites) from within the rift have assimilated lower crustal wall rock, probably because the background temperatures in the lower crust of the rift are higher and because these rocks are associated with large-volume, long-lived volcanic fields that locally enhance thermal input into the lower crust. Lithospheric mantle of the Rio Grande rift region is younger than lithospheric mantle beneath the Archean craton to the north (1.7 versus 2.7 b.y. old), which is compatible with the higher ε_{Nd} values of EM-derived volcanic rocks of the rift region. A "plum pudding" model of the mantle, in which the least refractory, more incompatible-element-enriched heterogeneities preferentially determine the isotopic composition of melts, can account for the isotopic compositions of basalts in the rift region.

INTRODUCTION

Continental and mid-ocean ridge (MOR) tholeiites are typically different in their chemical and isotopic compositions [e.g., *DePaolo and Wasserburg*, 1976*a*, 1979*a*; *Allègre* et al., 1982; *Dupuy and Dostal*, 1984]. Debate has centered on whether these differences are due to crustal interaction or whether they reflect differences between subcontinental and suboceanic mantle source regions. Continental alkali basalts, on the other hand, are frequently geochemically indistinguishable from oceanic alkali basalts, evidence that suboceanic-type mantle (i.e., asthenosphere) is a source of basalts beneath some continental areas [e.g., *DePaolo and Wasserburg*, 1976*a*; *Allègre et al.*, 1981; *Fitton and Dunlop*, 1985].

In the western United States, late Cenozoic extension has thinned much of the continental lithosphere, resulting in asthenospheric upwelling. Late Cenozoic volcanic rocks from several localities at the western continental margin and in the Basin and Range Province have Nd and Sr isotopic compositions typical of oceanic island basalts and appear to have been derived from the asthenosphere [*DePaolo and Wasserburg*, 1976*a*; *Carlson*, 1984; *Hart*, 1985; *Menzies et al.*, 1983, 1985]. In contrast, volcanic rocks from the continental interior of the western United States (eastern Columbia Plateau, Snake River Plain–Yellowstone, Leucite Hills, southern Great Plains, and Smoky Butte, Montana) have lower ε_{Nd} and higher $^{87}Sr/^{86}Sr$ compared to most oceanic island basalts [*Menzies et al.*, 1983; *Phelps et al.*, 1983; *Carlson*, 1984; *Vollmer et el.*,

Paper number 7B7001.
0148-0227/87/007B-7001$05.00

1984; *Hart*, 1985; *Fraser et al.*, 1986]. These volcanic rocks occur in areas underlain by Precambrian basement and thick lithosphere and are interpreted as being derived from lithospheric mantle that has a history of incompatible element enrichment and isolation from the underlying convecting asthenosphere [e.g., *Menzies et al.*, 1983; *Vollmer et al.*, 1984]. *Hart* [1985] concluded that tholeiites from the northwestern Great Basin were derived from either lithospheric or asthenospheric mantle or a mixture of the two, depending on geographic position. Volcanism in that area straddled the boundary between Archean craton to the east and much younger crust of the continental margin to the west.

In this paper we present Nd and Sr isotopic data and major and trace element data for late Cenozoic alkali basalts (sensu lato) and tholeiitic basalts from the Rio Grande rift and adjacent regions of New Mexico. The Rio Grande rift is bounded by the Colorado Plateau, Great Plains, southern Rocky Mountains, and Basin and Range provinces and constitutes a unique geologic setting for studying the petrogenesis of continental basalts. In the rift and adjacent Basin and Range, where extension has disrupted the lithosphere, the asthenosphere has probably been involved in basalt generation. In adjoining areas of tectonic stability (Colorado Plateau and Great Plains), lithospheric mantle was the probable source of basalts. The primary purpose of this study is to determine, using basalts as probes of mantle chemistry, the characteristics and configuration of magma sources beneath the rift and adjoining provinces. The coexistence of alkalic and tholeiitic basalts, which may have sampled the mantle at different depths, also provides an opportunity to search for vertical variations in magma source regions within particular tectonic settings. Last, the rift region is suitable for examining the importance of crustal interaction in the petrogenesis of different basalt types from different tectonic settings.

GEOLOGIC SETTING

The Rio Grande rift, which is expressed morphologically as a series of en echelon, fault-bounded basins extending from central Colorado through New Mexico (Figure 1, inset), resulted from middle and late Cenozoic extensional deformation. The northern and central parts of the rift form a narrow, well-defined series of axial grabens that separate the stable platform of the Colorado Plateau from the craton of the Great Plains. The southern rift is a less distinct tectonic feature that merges with the southeastern Basin and Range. The rift is widest in the south where the earliest and greatest amount of extension occurred [*Chapin*, 1979; *Cordell*, 1982; *Seager et al.*, 1984]. The Precambrian basement of the rift region consists mainly of terranes of two ages, a 1.69- to 1.78-b.y.-old terrane beneath Colorado, northern New Mexico, and northern Arizona and a slightly younger 1.61- to 1.68-b.y.-old terrane beneath southern New Mexico and southern Arizona [*Van Schmus and Bickford*, 1981].

The lithospheric structure of the rift region can be inferred from geophysical studies [e.g., *Stewart and Pakiser*, 1962; *Roller*, 1965; *Warren*, 1969; *Toppozada and Sanford*, 1976; *Cordell*, 1978; *Keller at al.*, 1979*a*, *b*; *Olsen et al.*, 1979; *Ander*, 1981; *Daggett et al.*, 1981; *Sinno et al.*, 1986]. The crust of the Rio Grande rift and southeastern Basin and Range (generally 30–35 km thick) is thinner than the crust of the Colorado Plateau (40–45 km) or Great Plains (50 km). In addition, the crust of the northern rift is about 5 km thicker than that of the southern rift [*Toppozada and Sanford*, 1976; *Keller et al.*, 1979*b*; *Sinno et al.*, 1986], consistent with a greater amount of crustal extension in the southern rift. Total lithospheric thickness in the rift region is more difficult to determine but probably correlates with crustal thickness. Thermal and gravity modeling [*Keller et al.*, 1979*a*] suggest that the thickness of lithosphere beneath the Great Plains is approximately 100 km. Upper mantle P_n velocities beneath the Great Plains (8.2 km/s [*Stewart and Pakiser*, 1962]) are typical of "cold" lithosphere beneath stable continental areas and are consistent with the presence of thick subcrustal lithosphere. The lithosphere of the Colorado Plateau has been modeled as approximately 60 km thick [*Keller et al.*, 1979*a*]. However, upper mantle P_n velocities beneath the Colorado Plateau (7.8 km/s [*Roller*, 1965]) are lower than those beneath the Great Plains, suggesting that the upper mantle is hotter and more "asthenospheric" in its properties. Lithospheric thickness beneath the Rio Grande rift, southern Basin and Range, and the southeastern Colorado Plateau margin adjacent to the rift is generally interpreted [e.g., *Keller et al.*, 1979*a*; *Sinno et al.*, 1986; *Olsen et al.*, 1987] as coinciding with crustal thickness (i.e., the asthenosphere is in direct contact with the base of the crust with little or no intervening lithospheric mantle).

Volcanism in the Rio Grande rift region during the last 10 m.y. has been dominantly basaltic [*Luedke and Smith*, 1978], but significant volumes of intermediate and silicic rocks occur locally (e.g., Jemez and Mount Taylor volcanic fields, Figure 1). Most of the volcanism in the rift region was controlled not by the rift, but rather by the Jemez lineament, a northeast trending alignment of late Cenozoic volcanic fields that extends from the San Carlos volcanic field of Arizona to the Raton-Clayton volcanic field of northeastern New Mexico, a distance of about 700 km [*Mayo*, 1958; *Laughlin et al.*, 1976; *Smith and Luedke*, 1984]. The tectonic boundary between the Basin and Range Province and the southeastern Colorado Plateau lies within the interior of the physiographic plateau and is coincident with the Colorado Plateau portion of the Jemez lineament (Figure 1). That part of the Colorado Plateau southeast of, and including, the Jemez lineament is "transitional" in its upper crustal structure and lithospheric properties and is part of a broad transition zone concentric about the Colorado Plateau on the southeast, southwest, and west [*Thompson and Zoback*, 1979; *Zoback and Zoback*, 1980; *Ander*, 1981; *Baldridge et al.*, 1983; *Aldrich and Laughlin*, 1984].

Mafic volcanic rocks of the rift region encompass a spectrum of compositions that include nephelinite, basanite, alkali olivine basalt, hawaiite, mugearite, and olivine tholeiite. Compositions do not correlate consistently with tectonic setting, although there is a tendency for the most alkalic (and undersaturated) compositions to occur in volcanic fields outside the rift axis [*Lipman and Mehnert*, 1975; *Dungan et al.*, 1983; *Olsen et al.*, 1987]. Both tholeiitic and mildly alkalic lavas have erupted within the rift axis as well as on the rift flanks (mainly along the Jemez lineament) and commonly occur within the same volcanic field [e.g., *Lipman*, 1969; *Lipman and Moench*, 1972; *Laughlin et al.*, 1972, 1982; *Stormer*, 1972; *Lipman and Mehnert*, 1975, 1979*a*; *Aoki and Kudo*, 1976; *Baldridge*, 1979; *Baldridge et al.*, 1987].

ANALYTICAL PROCEDURES AND DATA REPRESENTATION

Isotopic data for Nd is given in terms of ε_{Nd} [*DePaolo and Wasserburg*, 1976*b*, 1977], the deviation in parts in 10^4 of the

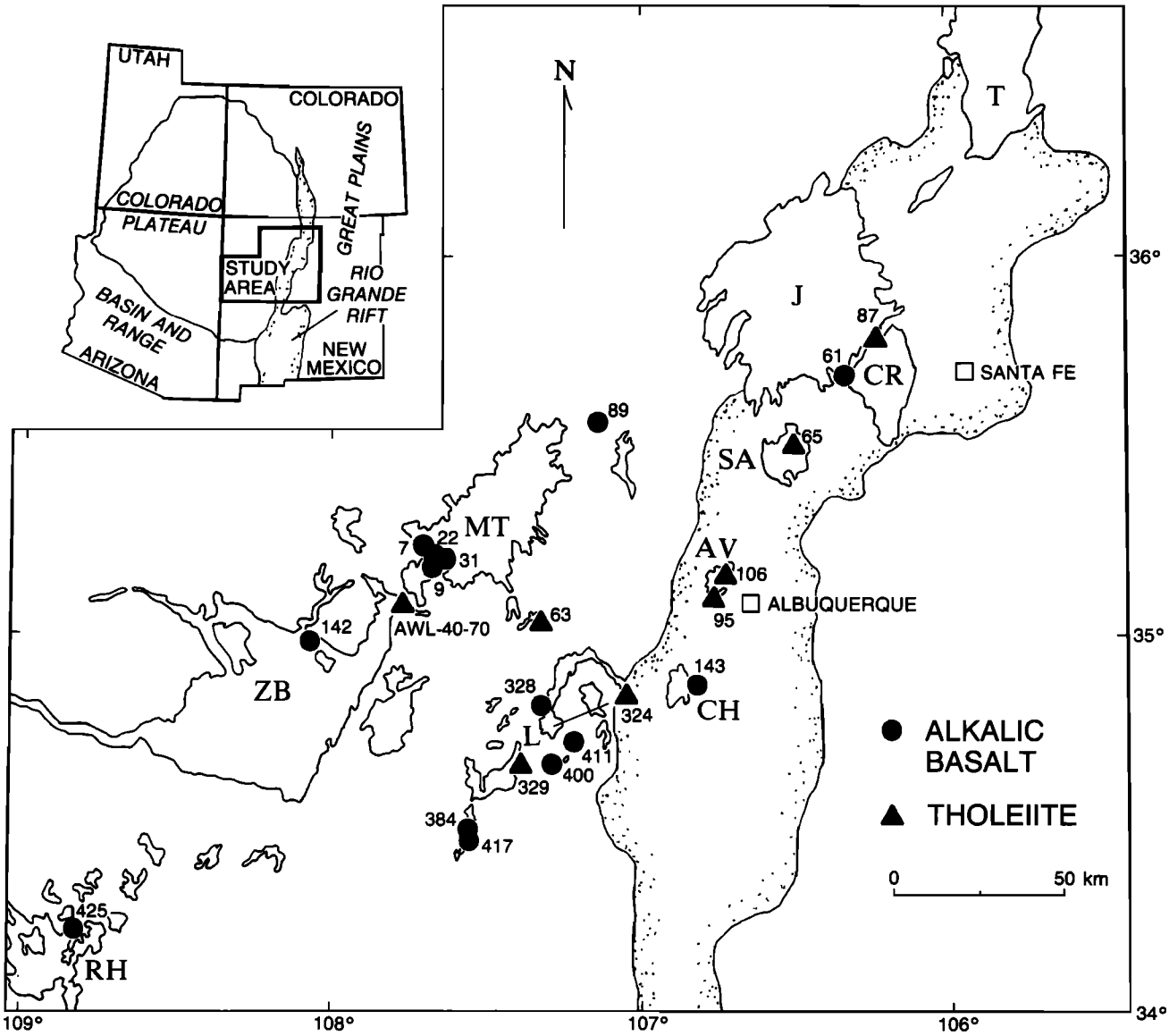

Fig. 1. Basalt sample localities and volcanic fields of the Rio Grande rift and the Colorado Plateau–Basin and Range transition zone. Sample numbers are given next to localities. Volcanic fields are T, Taos Plateau; J, Jemez Mountains; CR, Cerros del Rio; SA, Santa Ana Mesa; AV, Albuquerque Volcanoes; CH, Cat Hills; L, Lucero area; Mt, Mount Taylor; ZB, Zuni-Bandera; and RH, Red Hill. The Jemez lineament is marked by the RH, ZB, MT, J, and T volcanic fields. Line in the Lucero area connects sample 324 to its vent location. After *Baldridge et al.* [1983].

initial $^{143}Nd/^{144}Nd$ of the sample from the $^{143}Nd/^{144}Nd$ of a model chondritic reservoir (CHUR):

$$\varepsilon_{Nd} = 10^4 \left[\frac{^{143}Nd/^{144}Nd_{rock}}{^{143}Nd/^{144}Nd_{CHUR}} - 1 \right]$$

where $^{143}Nd/^{144}Nd_{CHUR}(today) = 0.511836$. Reference to ε_{Nd} and $^{87}Sr/^{86}Sr$ will always be to the initial values. No age correction of measured isotopic ratios was needed due to the young age of the samples and their low Rb/Sr and Sm/Nd ratios. The Sm/Nd enrichment factor, $f_{Sm/Nd}$, is defined as

$$f_{Sm/Nd} = (^{147}Sm/^{144}Nd_{rock}/0.1967) - 1$$

Nd and Sr isotopic measurements and analysis of Nd, Sm, Sr, and Rb (by isotope dilution) were made at the University of California, Los Angeles (UCLA) and at the Los Alamos National Laboratory. Procedures used at UCLA are described by *DePaolo* [1981*a*] except that Nd was measured as a NdO^+ rather than as a Nd^+ ion beam. Analyses at Los Alamos were performed on a 12-inch radius National Bureau of Standards (NBS)-style mass spectrometer in which Nd was measured as Nd^+. Nd isotopic compositions were fractionation-corrected to $^{146}Nd/^{142}Nd = 0.63613$ and Sr isotopic compositions to $^{86}Sr/^{88}Sr = 0.1194$. The precisions for Nd and Sr isotopic measurements are reported as the 2σ of the mean for an individual data collection run and reflect the internal precision within a particular run. Four analyses of the NBS 987 Sr standard at Los Alamos gave $^{87}Sr/^{86}Sr = 0.71015 \pm 2$, 0.71012 ± 3, 0.71012 ± 2, and 0.71004 ± 3, giving a mean value of 0.71011 ± 9 (2σ of four runs), which compares with a mean value of 0.71028 ± 3 (2σ of four runs) obtained at UCLA. For equivalency, all of the Los Alamos data (Table 2) and data discussed from the literature were normalized to NBS 987 = 0.71028. A replicate analysis of sample 143 (Table 2) done at Los Alamos gave a normalized $^{87}Sr/^{86}Sr$ value of

TABLE 1. Major Element, Trace Element, and Cation Normative Compositions of Rio Grande Rift Region Basalts

	Sample																					
	7	22	9	31	328	384	417	400	411	89	142	425	143	61	63	AWL-40-70	324	329	95	106	65	87
Type[a]	AB	AB	AB	AB	AB	AB	AB	AB	AB	AB	AB	AB	AB	AB	OT	OT	OT	OT	OT	OT	OT	OT
SiO_2	47.72	47.90	43.43	51.15	46.88	46.23	46.18	45.04	45.18	46.55	44.98	48.95	48.38	46.99	50.00	50.23	49.91	50.28	50.05	49.77	50.14	51.01
TiO_2	2.77	2.11	4.08	2.27	2.21	2.34	2.29	2.23	2.22	2.08	2.32	2.51	1.81	1.49	1.29	1.53	1.49	1.45	1.46	1.45	1.49	1.48
Al_2O_3	15.17	15.39	13.70	17.21	15.89	15.60	15.15	13.29	14.34	15.05	14.76	12.67	15.18	15.33	15.13	14.50	14.90	15.48	14.93	14.48	15.97	15.92
Fe_2O_3[b]	1.90	1.75	2.43	1.52	1.69	1.67	1.89	1.59	1.77	1.74	1.85	1.63	1.84	1.61	1.89	1.82	1.87	1.73	1.76	1.80	1.62	1.70
FeO	9.70	8.92	12.39	7.76	8.64	8.49	9.62	8.11	9.05	8.87	9.46	8.29	9.38	8.19	9.65	9.27	9.55	8.81	9.00	9.16	8.28	8.68
MnO	0.17	0.16	0.21	0.15	0.19	0.18	0.18	0.17	0.16	0.16	0.17	0.15	0.17	0.15	0.18	0.17	0.16	0.14	0.16	0.15	0.15	0.17
MgO	7.26	8.46	5.68	3.85	5.34	7.66	8.44	9.62	9.92	8.56	10.32	10.33	7.92	8.45	8.73	9.45	8.69	7.60	8.85	8.49	7.04	7.14
CaO	8.42	8.59	7.71	7.49	7.67	8.52	8.41	10.55	10.24	8.60	9.16	8.36	9.12	9.47	8.97	8.83	8.67	9.55	9.21	9.65	8.85	8.89
Na_2O	3.22	3.47	4.56	4.14	4.91	3.70	3.57	3.93	2.78	4.42	3.96	3.27	2.89	3.13	2.86	2.91	2.49	2.86	2.34	2.25	2.94	3.33
K_2O	1.38	1.58	2.42	1.88	1.51	1.53	1.48	1.30	1.52	1.57	1.47	1.92	1.09	1.12	0.61	0.77	0.70	0.81	0.60	0.51	1.26	1.11
P_2O_5	0.59	0.57	1.09	0.76	0.73	0.65	0.66	0.50	0.47	0.53	0.49	0.51	0.37	0.68	0.15	0.22	0.20	0.22	0.22	0.24	0.40	0.27
Total	98.30	98.90	97.70	98.18	95.66	96.57	97.87	96.33	97.65	98.13	98.94	98.59	98.15	96.61	99.46	99.70	98.63	98.93	98.58	97.95	98.14	99.70
Q	0.00	0.00	0.00	0.00	0.00	0.00	0.00	0.00	0.00	0.00	0.00	0.00	0.00	0.00	0.00	0.00	0.00	0.00	0.00	0.03	0.00	0.00
or	8.33	9.37	14.76	11.34	9.25	9.29	8.88	7.83	9.12	9.30	8.62	11.38	6.57	6.79	3.62	4.54	4.20	4.84	3.60	3.09	7.58	6.57
ab	29.53	26.02	15.96	37.96	29.89	24.80	23.60	12.88	14.21	19.57	12.72	26.46	26.46	26.83	25.79	26.10	22.72	25.98	21.35	20.72	26.90	29.94
an	23.36	21.84	10.08	23.31	17.48	22.03	21.27	15.08	22.52	16.63	18.03	14.27	25.73	25.12	26.76	24.21	27.86	27.33	28.92	28.62	27.17	25.25
ne	0.00	3.15	15.79	0.00	9.48	5.60	5.37	13.87	6.69	12.13	13.55	1.80	0.00	1.21	0.00	0.00	0.00	0.00	0.00	0.00	0.00	0.00
di	12.30	13.76	17.64	7.65	13.62	13.63	13.38	27.99	20.79	18.14	19.14	19.20	14.36	14.84	13.56	14.50	11.62	15.32	12.84	15.10	11.93	13.72
hy	3.09	0.00	0.00	7.34	0.00	0.00	0.00	0.00	0.00	0.00	0.00	0.00	7.28	0.00	15.91	14.58	25.04	15.77	27.04	27.92	15.30	10.41
ol	16.17	19.88	14.93	5.92	13.68	18.12	20.86	16.41	20.65	18.39	21.79	20.61	14.28	19.89	10.26	11.58	4.04	6.43	1.85	0.00	6.44	9.71
mt	2.03	1.84	2.62	1.62	1.83	1.79	2.01	1.70	1.88	1.82	1.92	1.71	1.96	1.72	1.98	1.90	1.99	1.83	1.87	1.93	1.73	1.78
il	3.94	2.95	5.87	3.23	3.19	3.35	3.24	3.17	3.14	2.90	3.21	3.51	2.57	2.13	1.80	2.13	2.11	2.04	2.07	2.07	2.11	2.06
ap	1.26	1.20	2.35	1.62	1.58	1.40	1.40	1.07	1.00	1.11	1.02	1.07	0.79	1.46	0.31	0.46	0.42	0.47	0.47	0.51	0.85	0.57
Mg #[b]	57.2	62.8	45.0	46.9	52.4	61.7	61.0	67.9	66.1	63.2	66.0	68.9	60.1	64.8	61.7	64.5	61.9	60.6	63.7	62.3	60.3	59.4
Sr	721	827	1189	771	995	712	688	676	1177	1173	664	671	490	934	240	331	317	368	312	300	640	431
Rb	24.8	25.6	48.2	30.7	36.0	23.4	25.3	17.8	31.8	22.8	17.1	39.4	9.4	15.9	12.9	15.2	16.3	15.2	11.5	7.4	21.7	18.1
Nd	34.1	32.6	69.0	41.6	43.4	29.6	29.6	37.2	32.8	36.9	28.4	36.2	19.0	39.1	12.5	17.2	15.2	16.3	13.5	12.8	27.4	20.7
Sm	7.17	6.93	12.86	8.56	7.78	6.21	6.25	7.26	6.61	7.48	6.03	7.72	4.44	6.87	3.24	4.21	3.88	4.10	3.48	3.32	5.46	4.65
Zr	240	226	459	285	386	224	215	235	253	272	208	227	185	272	103	132	127	139	115	110	200	149
Cr	149	207	27	58	59	145	175	429	354	230	237	273	255	220	233	272	235	254	273	206	181	223

[a]AB, alkali basalt; OT, olivine tholeiite.
[b]Fe_2O_3 and Mg # [100 × Mg/(Mg + Fe^{2+})] calculated assuming Fe^{3+}/total Fe = 0.15.

TABLE 2. Nd and Sr Isotopic Compositions and Ages of Rio Grande Rift Region Basalts

Sample	Type[a]	Age, m.y.	Sm/Nd	Rb/Sr	$^{87}Sr/^{86}Sr$	$^{143}Nd/^{144}Nd$	ε_{Nd}
7[b]	AB	2.89[c]	0.210	0.034	0.70369 ± 3	0.512052 ± 27	+4.2
22[b]	AB	2.01[c]	0.213	0.031	0.70366 ± 3	0.512091 ± 18	+5.0
9[b]	AB	3.73[c]	0.186	0.041	0.70354 ± 2	0.512065 ± 21	+4.5
31[b]	AB	<3	0.206	0.040	0.70377 ± 3	0.512047 ± 21	+4.1
328[b]	AB	0.8[d]	0.179	0.036	0.70343 ± 3	0.512120 ± 20	+5.5
384	AB	~4[d]	0.210	0.033	0.70320 ± 2	0.512150 ± 15	+6.1
417	AB	4.3[d]	0.211	0.037	0.70306 ± 3	0.512173 ± 16	+6.6
400	AB	7.7–7.9[d]	0.195	0.026	0.70442 ± 2	0.512003 ± 19	+3.3
411	AB	7.2[e]	0.201	0.027	0.70614 ± 3	0.512053 ± 20	+4.2
89	AB	<5	0.203	0.019	0.70557 ± 3	0.512096 ± 20	+5.1
142	AB	<0.2[f]	0.212	0.026	0.70366 ± 2	0.512115 ± 23	+5.4
425	AB	<5	0.213	0.059	0.70371 ± 2	0.512045 ± 31	+4.1
143[b]	AB	0.14[g]	0.234	0.019	0.70392 ± 3	0.512080 ± 24	+4.8
61	AB	2–3	0.176	0.017	0.70410 ± 1	0.511950 ± 18	+2.2
63	OT	0.38[h]	0.260	0.054	0.70594 ± 2	0.511892 ± 23	+1.1
AWL-40-70	OT	0.05[i]	0.244	0.046	0.70521 ± 1	0.511910 ± 22	+1.4
324[b]	OT	0.32[e]	0.256	0.051	0.70636 ± 3	0.511822 ± 16	−0.3
329	OT	3.4[d]	0.252	0.041	0.70589 ± 2	0.511866 ± 12	+0.6
95	OT	0.19[e]	0.259	0.037	0.70451 ± 2	0.512047 ± 20	+4.1
106	OT	0.19[e]	0.260	0.025	0.70386 ± 2	0.512079 ± 23	+4.8
65	OT	2–3	0.199	0.034	0.70459 ± 1	0.511900 ± 28	+1.2
87	OT	2–3	0.225	0.042	0.70476 ± 3	0.511865 ± 20	+0.6

[a]AB, alkali basalt; OT, olivine tholeiite.
[b]Isotopic and isotope dilution measurements done at UCLA.
[c]F. V. Perry and M. Shafiqullah (unpublished data, 1987).
[d]*Baldridge et al.* [1987].
[e]*Bachman and Mehnert* [1978].
[f]*Laughlin et al.* [1979].
[g]*Kudo et al.* [1977].
[h]*Lipman and Mehnert* [1979*b*].
[i]A. W. Laughlin and M. Shafiqullah (unpublished data, 1987).

0.70389 ± 2 which compares to a value of 0.70392 ± 3 obtained at UCLA. Two analyses of a UCLA Nd normal (ε_{Nd} = −17.29 ± 0.40, measured at UCLA) gave ε_{Nd} = −17.52 ± 0.48 and −16.97 ± 0.28 at Los Alamos during the period of data collection for this study. Five measurments of the UCLA Nd normal done previous to the period of data collection (by another operator) gave a mean ε_{Nd} value of −17.17 ± 0.95 (2σ of five runs) and a range of −16.63 ± 0.52 to −17.65 ± 0.32. We are reasonably confident that the ε_{Nd} values determined for this study are accurate to within about 0.5 ε units. Replicate isotope dilution measurements indicate a precision of about 1% for Nd, Sm, Sr, and Rb. Total procedural blanks at Los Alamos and UCLA were, respectively, 0.46, and 0.40 ng for Nd, 0.06 and 0.13 ng for Sm, 4.6 and 4.6 ng for Sr, and 1.8 and 0.9 ng for Rb, all of which are negligible for these rocks.

Major element, Zr, and Cr concentrations were obtained by X ray fluorescence analysis at the Los Alamos National Laboratory using procedures described by *Vaniman et al.* [1985]. Precisions for Zr and Cr are 3–5% and 5–10%, respectively.

In general, we follow the terminology of *Yoder and Tilley* [1962] and *Irvine and Baragar* [1971] in classifying basalts as tholeiitic or alkalic. However, some of the hy-normative basalts lie in the alkali olivine basalt field of *Irvine and Baragar* [1971] and are more similar to the alkalic (i.e., ne-normative) rocks in their major and trace element compositions (and, we infer, in their petrogenesis) than to other hy-normative (tholeiitic) basalts. Therefore, in contrast to previous studies in the area [e.g., *Baldridge*, 1979; *Baldridge et al.*, 1982], we classify them with the alkali basalts.

RESULTS

We have analyzed the major and trace element compositions and Nd and Sr isotopic compositions of 22 alkalic and tholeiitic basalts from the Rio Grande rift and the adjacent Colorado Plateau–Basin and Range transition zone (Figure 1 and Tables 1 and 2). Samples were chosen to represent the major compositional group(s) within individual volcanic fields, and we generally chose the least evolved basalts within a compositional group of a volcanic field. The ages of all of the samples are reasonably well known, either from K-Ar dates or from geologic relationships (Table 2). Except for two alkali basalts that are between 7 and 8 m.y. old, all of the basalts samples are <5 m.y. old. Major element compositions of the basalts (Figure 2) include most of the basalt compositions found in the area of Figure 1. All of the tholeiites have >10% normative hypersthene, while the normative compositions of the alkali basalts range from 16% nepheline to 7% hypersthene (Figure 3 and Table 1).

Major Elements

SiO_2 content of the alkali basalts ranges from 43 to 51 wt %, covering a large compositional range that includes basanite, alkali olivine basalt, ne-normative hawaiite, and hy-normative hawaiite. Mg numbers (100 × Mg/(Mg + Fe^{2+})) of the alkali basalts (adjusted to Fe^{3+}/total Fe = 0.15) range from 45 to 69, with most values greater than 60. Basalts with Mg numbers ≥ 68 probably represent primary mantle magmas that were in equilibrium with upper mantle olivine compositions and subsequently erupted at the surface without

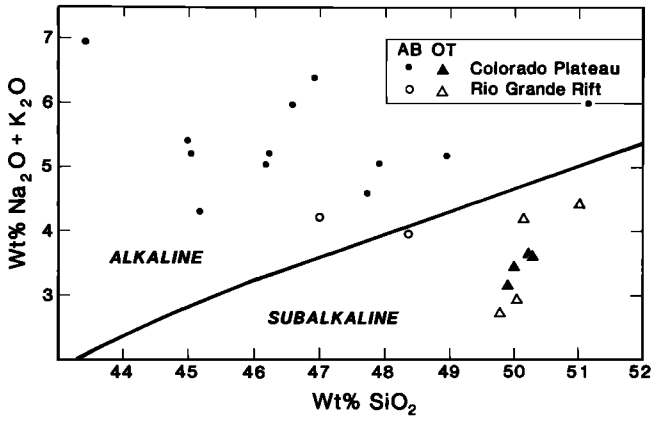

Fig. 2. Alkalis versus silica for basalts of the Rio Grande rift region. "AB" and "OT" in legend are alkali basalt and olivine tholeiite, respectively. Line separating alkaline from subalkaline fields is from *Irvine and Baragar* [1971].

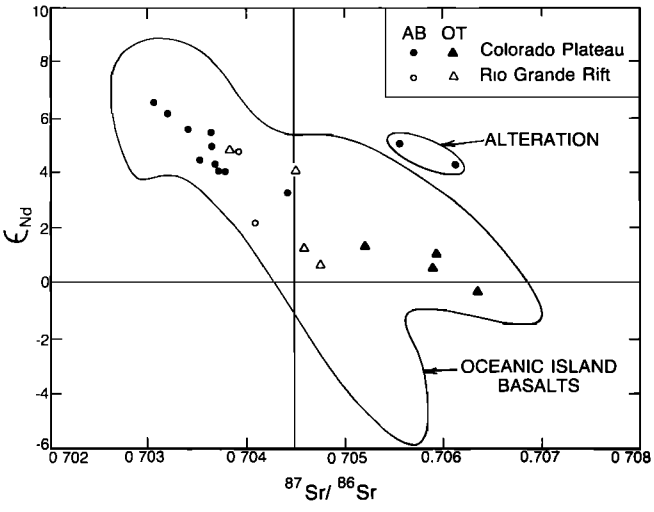

Fig. 4. Initial ε_{Nd} versus $^{87}Sr/^{86}Sr$ for alkali basalts (AB) and olivine tholeiites (OT) of the Rio Grande rift and Colorado Plateau transition zone measured in this study. Field for oceanic island basalts is from *White* [1985]. Altered samples are discussed in text.

significant compositional modification [e.g., *Frey et al.*, 1978]. Two alkali basalts (22 and 89) contain spinel lherzolite xenoliths, indicating rapid ascent from the mantle. Both have Mg numbers of 63, which suggests that some crystal fractionation may have taken place within the upper mantle before incorporation of the xenoliths.

Tholeiites encompass a relatively narrow compositional range (Figure 2), with SiO_2 of 49.8–51 wt % and Mg numbers of 59–65. Normative hypersthene ranges from 10 to 28%, with one sample (106) having a small amount of normative quartz. The tholeiites from the Colorado Plateau transition zone and the central Rio Grande rift form a distinct, compositionally homogeneous group having uniformly low alkali content (low-alkali tholeiites: $Na_2O + K_2O < 4\%$), while tholeiites from farther north in the rift (65 and 87) have a higher total alkali content (high-alkali tholeiites: $Na_2O + K_2O > 4\%$).

Trace Elements

All of the basalts are light rare earth element (LREE) enriched, which we infer from the fact that measured Sm/Nd ratios (Table 2) are lower than the chondritic value (0.325). Generally, the alkali basalts have lower Sm/Nd and higher Nd, Sm, Rb, Sr, and Zr concentrations than the tholeiites. Low-alkali tholeiites are relatively homogeneous in their trace element content. The Cr, Zr, Nd, Sm, and Sr contents of all samples are similar within a factor of 1.5. Rb has the greatest range among the low-alkali tholeiites (7.4–16.3 ppm). High-alkali tholeiites are enriched relative to low-alkali tholeiites in Nd, Sm, Rb, Sr, and Zr and have lower Sm/Nd. All of the tholeiites are enriched in incompatible trace elements compared to normal MOR tholeiites [e.g., *Sun et al.*, 1979].

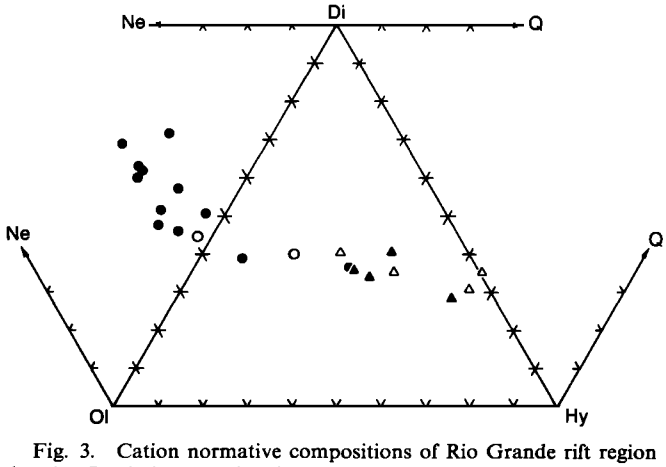

Fig. 3. Cation normative compositions of Rio Grande rift region basalts. Symbols are as in Figure 2. Note that sample 31, an evolved alkali basalt with Mg number = 47 (Table 1), plots with the tholeiites in this projection because of its low normative olivine content.

Nd and Sr Isotopes

Basalts from the Colorado Plateau transition zone define two distinct isotopic groups, one composed of alkali basalts and the other of tholeiites (Figure 4). Alkali basalts lie in the upper left quadrant of the Nd-Sr diagram ($\varepsilon_{Nd} = +6.6$ to $+3.3$; $^{87}Sr/^{86}Sr = 0.70306$ to 0.70442). Two altered alkali basalts (discussed below) have substantially higher $^{87}Sr/^{86}Sr$. All of the low-alkali tholeiites from the transition zone have lower ε_{Nd} and higher $^{87}Sr/^{86}Sr$ compared to the unaltered alkali basalts. The ε_{Nd} values of the tholeiites range from $+1.4$ to -0.3 and $^{87}Sr/^{86}Sr$ ranges from 0.70521 to 0.70636.

Basalts from the Rio Grande rift are more complicated in their isotopic values. Two different alkali basalts from the Rio Grande rift have been analyzed: (1) an alkali basalt (61) from the Cerros del Rio field in the northern rift is distinguished from alkali basalts of the Colorado Plateau transition zone by lower ε_{Nd} ($+2.2$) and higher $^{87}Sr/^{86}Sr$ (0.70410), and (2) an alkali basalt (143) from farther south in the rift has higher ε_{Nd} ($+4.8$) and lower $^{87}Sr/^{86}Sr$ (0.70392), similar to alkali basalts of the transition zone. The tholeiites that we have measured from the Rio Grande rift also fall into two isotopic groups: (1) high-alkali tholeiites from the Cerros del Rio and Santa Ana Mesa fields (65 and 87) are similar in ε_{Nd} to tholeiites of the Colorado Plateau transition zone but have lower $^{87}Sr/^{86}Sr$, and (2) low-alkali tholeiites from the Albuquerque Volcanoes (95 and 106) are simliar in ε_{Nd} to alkali basalts from the transition zone but have slightly higher $^{87}Sr/^{86}Sr$.

Alteration

Two alkali basalts (89 and 411) from the Colorado Plateau transition zone have substantially higher $^{87}Sr/^{86}Sr$ (0.70557 and 0.70614) compared to the rest of the alkali basalts but similar ε_{Nd} values (Figure 4). This higher $^{87}Sr/^{86}Sr$ correlates

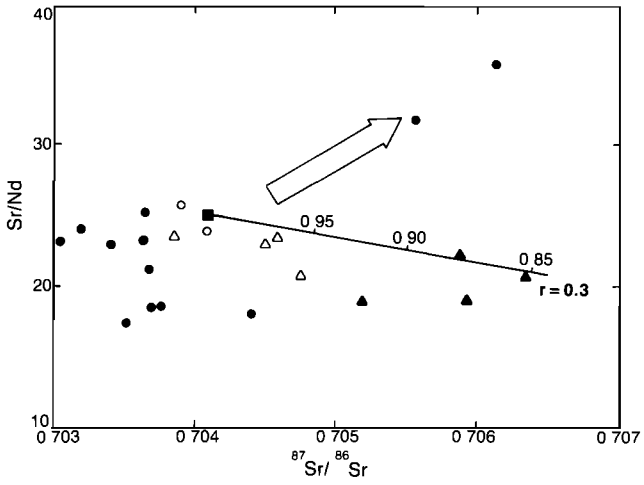

Fig. 5. Sr/Nd versus $^{87}Sr/^{86}Sr$ for Rio Grande rift region basalts. Symbols are as in Figure 2. Arrow indicates the trend produced by interaction of basalts with low-temperature groundwater high in Sr. The trend to higher Sr/Nd produced by alteration is the opposite of that produced by crustal assimilation. The curve shown is a model for crustal assimilation/fractional crystallization (parameters given in Figure 9 caption) that can account for the trace element and isotopic compositions of tholeiites as discused in the text.

with higher Sr/Nd (Figure 5), which we interpret as indicating secondary alteration by high Sr/Nd, high $^{87}Sr/^{86}Sr$ groundwater. The trend to higher Sr/Nd is opposite to that expected for crustal contamination. In addition, both basalts have fairly high Mg numbers (63 and 66), and sample 89 carries spinel lherzolite xenoliths, so it is unlikely that any crustal contamination mechanism is responsible for their higher $^{87}Sr/^{86}Sr$. The high Sr contents of these samples (1200 ppm) reflect addition of 400–500 ppm Sr (by comparison with the other alkali basalts of similar overall composition). Sample 411 shows some petrographic evidence of alteration (carbonate and minor clay in the groundmass), but sample 89 is free of any visible secondary minerals. This suggests to us that at least in the case of sample 89, Sr was mainly added along grain boundaries by interaction with low-temperature groundwater. This added Sr might have been removed by leaching, which we did not attempt. Sample 411 is one of our oldest samples (7.2 m.y. old) and occurs within a thick stack of flows, while sample 89 is from a portion of a volcanic neck that at one time was below the ground surface. Both of these situations permitted prolonged groundwater interaction.

DISCUSSION

The range in isotopic values in basalts from the Rio Grande rift region requires that more than one isotopically distinct component was involved in their petrogenesis. *Lipman and Mehnert* [1975] proposed that late Cenozoic basalts from the Rio Grande rift region were derived from two distinct mantle sources. They observed that basalts from the southern Basin and Range have systematically lower $^{87}Sr/^{86}Sr$ than those from the northern Rio Grande rift region. The Basin and Range basalts, with $^{87}Sr/^{86}Sr$ comparable to many oceanic island basalts, were interpreted as being derived from upwelled asthenospheric mantle. They cited Sr and Pb isotopic data to suggest that basalts from the northern Rio Grande rift and adjacent areas were generated within ancient lithospheric mantle, signifying that asthenospheric upwelling in these areas was not sufficient to involve the asthenosphere in basalt genesis.

Our data on the Nd and Sr isotopic compositions of basalts from the Rio Grande rift region suggest that at least three isotopically distinct components were involved in their petrogenesis: two distinct mantle sources and upper or middle crust. We use the isotopic compositions of alkali basalts as a first constraint to evaluate the characteristics of the mantle source beneath the rift region because we are reasonably certain that the alkali basalts have not interacted with the crust.

Alkali Basalts: Configuration and Nature of Mantle Source Regions

Two observations suggest that the isotopic variations of the alkali basalts reflect those in the mantle source and are not due to crustal interaction. (1) Two alkali basalts which we analyzed (22 and 89) contain spinel lherzolite xenoliths, indicating rapid ascent through the crust with little opportunity for crustal interaction or crystal fractionation. These basalts have $\varepsilon_{Nd} = +5$, which falls in the middle of the isotopic range for the alkali basalts we measured ($\varepsilon_{Nd} = +6.6$ to $+2.2$). Other alkali basalts of the rift region that carry mantle xenoliths have ε_{Nd} ranging from $+8$ to $+1.4$ [*Zindler*, 1980; *Phelps et al.*, 1983], indicating that these isotopic variations are not due to crustal contamination. (2) Isotopic composition does not correlate with a fractionation indicator such as Mg number. For example, samples 61, 400, 411, and 425 have relatively primitive compositions with Mg numbers ranging from 65 to 69 but have among the lowest ε_{Nd} values (the closest to crustal values), ranging from $+4.2$ to $+2.2$. We cannot rule out crustal contamination of tholeiites using these arguments and will discuss their petrogenesis separately in the next section.

A fundamental observation of this study is that the Nd and Sr isotopic compositions of alkali basalts from the Rio Grande rift region vary systematically with geographic position. The ε_{Nd} values, for instance, generally decrease from south to north across the rift region (Figure 6). More importantly, isotopic values correlate with distinct tectonic settings that have undergone differing degrees of lithospheric deformation during rifting and Basin and Range extension (Figure 7 and 8 and Table 3). Mantle-xenolith-bearing alkali basalts from the southern

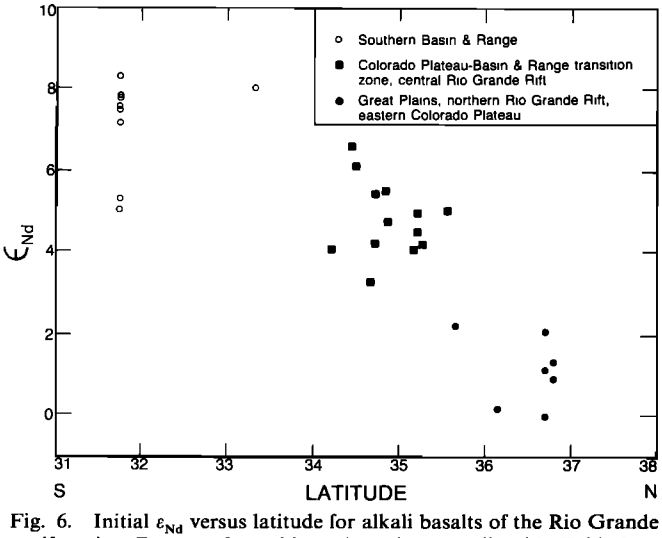

Fig. 6. Initial ε_{Nd} versus latitude for alkali basalts of the Rio Grande rift region. Data are from this study and sources listed in Table 3.

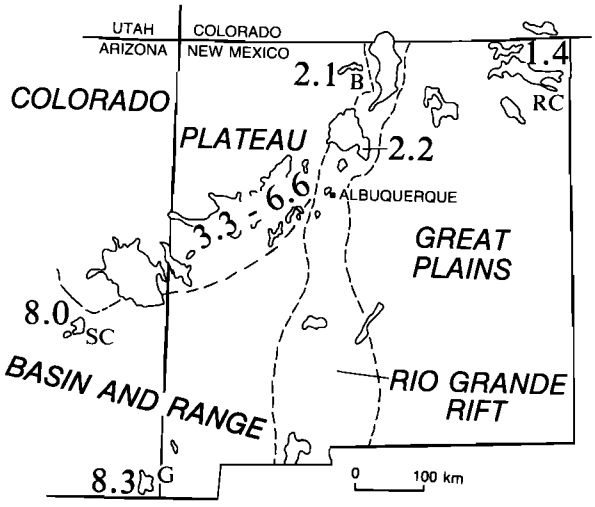

Fig. 7. Regional variation of ε_{Nd} for uncontaminated alkali basalts. Labeled volcanic fields are G, Geronimo; SC, San Carlos; B, Brazos; and RC, Raton-Clayton. Except for the range of values shown for alkali basalts of the Colorado Plateau transition zone, all of the ε_{Nd} values are the highest measured at any particular location. Data are from this study and sources listed in Table 3.

Basin and Range [*Zindler*, 1980; *Menzies et al.*, 1983, 1985] have the most MORB-like isotopic compositions in the rift region, clustering at ε_{Nd} values of +7 to +8. In contrast, alkali basalts from the eastern Colorado Plateau, northern Rio Grande rift, and Great Plains [*DePaolo and Wasserburg*, 1976*a*; *Phelps et al.*, 1983; *Williams*, 1984; this study], some of which also carry mantle xenoliths [*Phelps et al.*, 1983], have distinctly different isotopic compositions ($\varepsilon_{Nd} = 0$ to +2.2) compared to alkali basalts from the southern Basin and Range. Alkali basalts from the Colorado Plateau–Basin and Range transition zone and the central Rio Grande rift south of Santa Ana Mesa (Figure 1) have isotopic compositions of intermediate value (ε_{Nd} values of +3.3 to +6.6). These relationships suggest that two mantle "end-members" exist beneath the Rio Grande rift region and that the intermediate isotopic values of basalts from the Colorado Plateau–Basin and Range transition zone may represent a mixture of these two end-members. We refer to these isotopic end members as "depleted" mantle (DM), producing basalts with $\varepsilon_{Nd} = +7$ to +8, and "enriched" mantle (EM), producing basalts with $\varepsilon_{Nd} = 0$ to +2. The isotopic compositions of EM- and DM-derived alkali basalts indicate that EM has a history of lower Sm/Nd (LREE enrichment) and higher Rb/Sr relative to DM.

The geochemistry and isotopic compositions of alkali basalts from the Colorado Plateau transition zone are compatible with an origin involving mixing of DM and EM components (Figure 9). The small range in Sr/Nd of these alkali basalts (excluding altered samples), regardless of the relative DM or EM contribution (Figure 5), indicates that DM and EM also have siimilar Sr/Nd ratios. This is compatible with the approximately straight-line mixing relationship in the isotopic values (Figure 9).

The Nd and Sr isotopic compositions of alkali basalts in the rift region lie within the range of known oceanic island basalt isotopic compositions (Figure 8). Therefore the first hypothesis to consider in evaluating the configuration of the mantle source is that all of the alkali basalts in the rift region are derived from a single oceanic-type mantle source that is isotopically heterogeneous. If this hypothesis is correct, the source must be isotopically "zoned" from southwest to northeast, with DM concentrated beneath the southern Basin and Range and EM concentrated beneath the eastern Colorado Plateau, northern Rio Grande rift, and Great Plains. Large-scale regions with distinct isotopic characteristics have been recognized in the oceanic environment [*Dupré and Allègre*, 1983; *Hart*, 1984], and an analogous situation (on a smaller scale) may exist beneath the rift region.

An alternative to a single zoned source for the alkali basalts is a two-layer mantle, with DM and EM constituting different layers. We prefer this model for the rift region because of (1) the correspondence of distinct isotopic values for alkali basalts to certain tectonic settings, (2) the relationship of isotopic values to the lithospheric structure of the rift region known from geophysical studies, and (3) the way in which lithospheric structure and basalt source regions are modified by an evolving rift. We will amplify these arguments in the remainder of this section.

The Rayton-Clayton volcanic field lies on the Great Plains within the continental craton (Figure 7). The lithosphere beneath this part of the Great Plains is presumed, from gravity, heat flow, and seismic data, to be at least 100 km thick [*Keller et al.*, 1979*a*]. Basanites and nephelinites from the Raton-Clayton field have EM isotopic signatures and probably last equilibrated at depths of less than 100 kms [*Green*, 1970; *Bultitude and Green*, 1971]. Beneath the Great Plains, therefore, we assume that EM corresponds to lithospheric mantle. Lithospheric mantle characterized by a history of high Rb/Sr and low Sm/Nd and isolation from the underlying asthenosphere has been increasingly recognized as a source of continental volcanic rocks from the North American craton [e.g., *Menzies et al.*, 1983; *Vollmer et al.*, 1984; *Hart*, 1985, *Fraser et al.*, 1986].

In contrast to the thick lithosphere beneath the Great Plains, the lithosphere beneath the southern Basin and Range has been substantially thinned by extensional deformation. Anomalously low upper mantle P_n velocities of 7.8 km/s [*Warren*, 1969; *Gish et al.*, 1981] as well as thermal and gravity modeling [*Keller et al.*, 1979*a*] indicate that the asthenosphere beneath the southern Basin and Range is in contact with the base of the crust at a depth of 25–30 km. Therefore

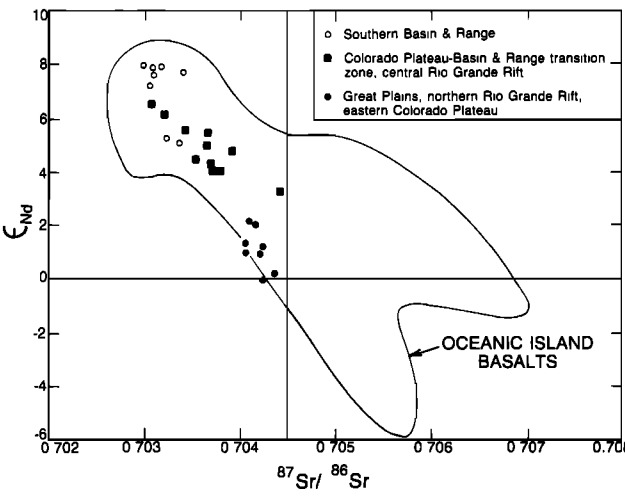

Fig. 8. Initial ε_{Nd} versus $^{87}Sr/^{86}Sr$ for uncontaminated alkali basalts of the Rio Grande rift region. Field for oceanic island basalts is from *White* [1985]. Data are from this study and sources listed in Table 3. Data for altered samples (Figure 4) are omitted.

TABLE 3. Summary of Nd and Sr Isotopic Compositions of Alkali Basalts From the Rio Grande Rift and Adjacent Regions

Tectonic Setting	Volcanic Field(s)	n	ε_{Nd}	$^{87}Sr/^{86}Sr$[a]	Reference
Southern Basin and Range	Geronimo	9	+8.3–+5.2	0.70298–0.70340	*Menzies et al.* [1983, 1985]
	San Carlos	1	+8.0	0.70298	*Zindler* [1980]
Colorado Plateau transition zone, central Rio Grande rift	see Figure 1	13	+6.6–+3.3	0.70306–0.70442[b]	this study
Northern Rio Grande rift, eastern Colorado Plateau, Great Plains	Jemez, Cerros del Rio	2	+2.2–+0.2	0.70410–0.70436	*DePaolo and Wasserburg* [1976a] and this study
	Brazos	3	+2.1–0	0.70417–0.70423	*Williams* [1984]
	Raton-Clayton	3	+1.4–+1.0	0.70406–0.70421	*Phelps et al.* [1983]

[a]All $^{87}Sr/^{86}Sr$ ratios are relative to NBS 987 = 0.71028.
[b]Does not include altered samples 89 and 411.

alkali basalts from this region probably equilibrated within the asthenosphere, and their DM isotopic signatures indicate that DM beneath this region corresponds to the asthenosphere.

We suggest that the DM/asthenosphere source beneath the southern Basin and Range is part of the convecting upper mantle present worldwide beneath both continents and oceans. The isotopic signature of DM ($\varepsilon_{ND} = +7$ to $+8$, $^{87}Sr/^{86}Sr \sim 0.7032$) corresponds to the PREMA ("prevalent mantle") component of *Zindler and Hart* [1986] and is an isotopic signature shared by a large number of oceanic island basalts, island arc basalts, and the most isotopically "depleted" continental basalts. It is clear, however, from isotopic measurements of oceanic basalts that the convecting upper mantle is chemically heterogeneous and includes both enriched and depleted components. A physically plausible means of accounting for upper mantle heterogeneity is a "plum pudding" model (or more accurately, in the case of convecting mantle, a "marble cake" model) in which small-scale, incompatible-element-enriched components (the plums) are scattered throughout an incompatible-element-depleted lherzolite matrix (the pudding) [e.g., *Zartman and Doe*, 1981; *Davies*, 1981, 1984; *Morris and Hart*, 1983; *Batiza*, 1984; *Gill*, 1984; *Zindler et al.*, 1984]. Isotopic variations on both large and small length scales could be due to variable concentrations of enriched components or differences in the nature of the enriched components within different volumes of mantle. The enriched components may represent any combination of basaltic intrusions, metasomatised lherzolite, subducted oceanic crust, recycled continental material, detached subcontinental lithosphere, or material transported from the lower mantle [e.g., *Zartman and Doe*, 1981; *Hofmann and White*, 1982; *McKenzie and O'Nions*, 1983; *Morris and Hart*, 1983; *Allègre et al.*, 1984; *Zindler et al.*, 1984].

According to the plum pudding model, the isotopic and trace element composition of a basalt depends on the relative proportion of enriched or depleted components that contribute to the melt. For a small percentage of melting (e.g., alkali basalts), the more enriched (and less refractory) components are preferentially incorporated into the melt. At a larger percentage of melting (e.g., MOR tholeiites), a larger proportion of depleted lherzolite contributes to the melt, diluting the enriched component and resulting in a more depleted trace element and isotopic signature. If the plum pudding model is correct for the DM source, the DM isotopic signature must represent a reproducible mixture of enriched and depleted components. This would probably require that the enriched heterogeneities be small (a scale length of meters to tens of meters) and evenly distributed so that DM beneath the rift region is "homogeneous" on a scale of kilometers. Partial melts within a certain percentage range that produces alkali basalts could then acquire a reproducible DM isotopic signature that represents the large-scale "homogeneity" of a source that is heterogeneous on a small scale.

The simplest two-layer source model for the Rio Grande rift region is that EM always corresponds to subcrustal lithosphere and the underlying DM always corresponds to asthenosphere. Where the lithosphere has not been extended (Great Plains), the lithospheric mantle remains intact and EM/lithosphere is the source of basalts. Where considerable extension has occurred (southern Basin and Range), the lithosphere has been thinned and the lithospheric mantle replaced by DM/asthenosphere.

The simple two-layer model is not valid for all areas of the rift region. For instance, gravity and seismic data suggest that the asthenosphere is in contact with the base of the crust beneath the axial grabens of the Rio Grande rift in both northern and southern New Mexico [*Olsen et al.*, 1979; *Baldridge et al.*, 1984; *Sinno et al.*, 1986; M. E. Ander, personal communication, 1986]. Below the eastern Colorado Plateau, mantle structure is less well known, but mantle P_n velocities (7.9 km/s [*Toppozada and Sanford*, 1976]) are similar to those beneath the rift (~7.7 km/s), suggesting that the asthenosphere here may also be near the base of the crust. Alkali basalts from the northern rift and eastern Colorado Plateau, however, have EM isotopic signatures. Likewise, anomalously low P_n velocities (7.7–7.8 km/s) beneath the southeastern Colorado Plateau–Basin and Range transition zone suggest that the asthenosphere is in contact with the base of the crust [*Baldridge et al.*, 1984; K. H. Olsen, personal communication, 1986]. Yet alkali basalts from the transition zone have Nd and Sr isotopic ratios that suggest a source containing both DM

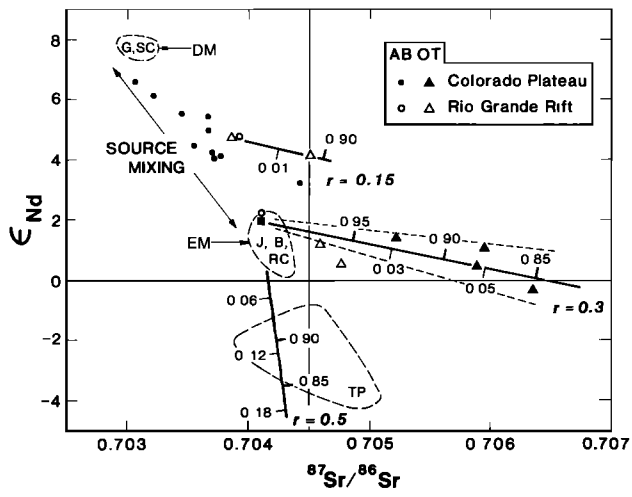

Fig. 9. Petrogenetic model for Rio Grande rift region basalts in terms of ε_{Nd} versus $^{87}Sr/^{86}Sr$. Altered alkali basalts shown in Figure 4 have been omitted. DM and EM fields encompass values of DM-derived alkali basalts from the Geronimo (G) and San Carlos (SC) volcanic fields, and EM-derived alkali basalts from the Jemez (J), Brazos (B), and Raton-Clayton (RC) volcanic fields (Table 3 and Figure 7). Alkali basalts from the Colorado Plateau transition zone and a tholeiite from the central Rio Grande rift define a mixing array between the DM and EM fields and were derived from the DM/EM boundary. Curves model fractional crystallization accompanied by crustal assimilation for mantle-derived magmas (AFC equations of *DePaolo* [1981*c*]). Upper tick marks along curves are values of F, the ratio of the final magma mass to the initial magma mass. Lower tick marks are values of $M_a/M_m{}^0$, the ratio of the mass assimilated to the initial mass of magma. Values of r of each curve are the ratio of the assimilation rate to the fractionation rate. The solid square within the EM field is a model value ($\varepsilon_{Nd} = +2$, $^{87}Sr/^{86}Sr = 0.7041$, Nd = 12 ppm, Sr = 300 ppm) for an EM-derived magma parental to the Colorado Plateau tholeiites and Taos Plateau tholeiites and alkali basalts (field labeled TP). The assimilation/fractional crystallization (AFC) curves for the Colorado Plateau tholeiites and Albuquerque Volcano tholeiites (upper curve) assume an upper crustal contaminant with $\varepsilon_{Nd} = -12$, $^{87}Sr/^{86}Sr = 0.735$, Nd = 30 ppm, Sr = 350 ppm. The dashed lines encompassing the Colorado Plateau tholeiites are the upper and lower bounds for several AFC curves that use a variety of upper crustal compositions as contaminants (see text and Figure 13, caption). A generalized AFC curve was calculated for Taos Plateau (TP) basalts assuming a Rb-depleted, lower crustal contaminant with $^{87}Sr/^{86}Sr = 0.705$, Sr = 450 ppm, $\varepsilon_{Nd} = -18$, Nd = 30 ppm, with the isotopic values being suggested by the isotopic compositions of crustally derived dacites from the Taos Plateau [*Williams*, 1984]. The higher r value for the Taos Plateau basalts is consistent with the contamination by hot lower crust.

and EM components. Thus some areas of the rift region, which have EM or partial EM isotopic signatures, are not detectably underlain by lithospheric mantle. Instead, the mantle beneath these areas has the geophysical properties of asthenosphere. This suggests that the asthenosphere/lithosphere boundary (a rheological boundary) does not correspond to a geochemical boundary between DM and EM in these areas. We emphasize that both the northern Rio Grande rift and the Colorado Plateau transition zone are at an intermediate stage of lithospheric extension compared to the Great Plains and the southern Basin and Range. Our interpretation is that the lithospheric mantle beneath the northern Rio Grande rift and the transition zone has been "thermally thinned," acquiring the geophysical properties (low P_n velocity and density) of asthenosphere but has not yet been completely replaced by chemically distinct DM. Therefore these sources have EM, or partial EM, isotopic signatures, but asthenospheric geophysical properties.

Mechanisms to account for lithospheric heating and thinning during rifting commonly assume an anomalous asthenospheric heat source such as a mantle plume [e.g., *Spohn and Schubert*, 1983; *Moretti and Froidevaux*, 1986]. However, anomalously high sublithospheric heat may not be required to thermally thin the lithosphere. *Buck* [1986] modeled lithospheric thinning through transport of heat into the lithosphere by small-scale asthenospheric convection induced by extension. Small-scale convection results from horizontal temperature gradients that develop beneath rifts as the lithosphere is thinned by extension, and hotter, upwelled asthenosphere is juxtaposed against colder lithosphere beneath the rift flanks. The amount of heat transported into the lithosphere by small-scale convection is greater than that transported by purely conductive heat transport. Thermal expansion of the lithosphere resulting from small-scale convection can account for the magnitude and distribution of flank uplift observed for many rifts [*Buck*, 1986]. Once lithosphere is thermally converted to asthenosphere, it can convectively mix with, and eventually be replaced by, DM/asthenosphere. This model of thermal thinning by small-scale convection is compatible with "passive" rifting and is probably more applicable to the Rio Grande rift than models postulating a deep-seated mantle heat source [e.g., *Baldridge et al.*, 1984; *Olsen et al.*, 1987]. Small-scale convection could also have been induced beneath the Colorado Plateau–Basin and Range transition zone as upwelled asthenosphere beneath the Basin and Range abutted against the lithosphere beneath the Colorado Plateau interior.

In order to relate the isotopic compositions of alkali basalts to the evolution and configuration of their source regions, we must first constrain the depth at which alkali basalts equilibrate in the mantle. Experimental work by *Takahashi* [1980] and *Takahashi and Kushiro* [1983] showed that alkali olivine basalts which are chemically similar to rift region alkali basalts equilibrate with the mantle assemblage olivine, clinopyroxene, and orthopyroxene at pressures of 14–20 kbar, equivalent to a depth of about 45–65 km. Although we consider this equilibration depth to be approximately correct for alkali basalts of the rift region, the absolute depth is not as important as the assumption that alkali basalts of similar composition, which occur in the northern rift, eastern Colorado Plateau, transition zone, and southern Basin and Range, equilibrated at similar PT conditions in the mantle and therefore at approximately the same depth (within a range of 20 km) beneath all tectonic provinces. We can think of no reason, for instance, why alkali basalts from the southern Basin and Range would have systematically equilibrated at a different depth than compositionally similar alkali basalts from the northern Rio Grande rift. Therefore the systematic isotopic differences of alkali basalts from different tectonic provinces, if not controlled by equilibration depth, must reflect different depths to the DM/EM boundary beneath these provinces.

We propose that the depth to the DM/EM and asthenosphere/lithosphere boundaries beneath different areas of the rift region reflects different evolutionary stages of rifting in each area (Figure 10). Prior to regional extensional deformation, the lithosphere is thick (~100 km) throughout the rift region, and the asthenosphere/lithosphere boundary coincides with the DM/EM boundary (Figure 10, stage 1). Thus DM corresponds to asthenosphere, and EM corresponds to lithospheric mantle. This situation still exists beneath the Great Plains. At an intermediate stage of rifting (northern Rio Grande rift) the lithosphere is thermally thinned, and the as-

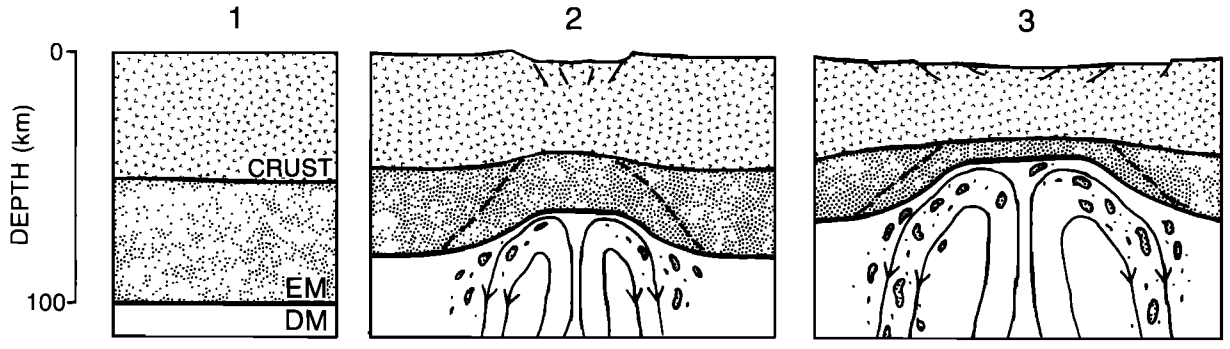

Fig. 10. Model depicting stages in the evolution of mantle sources and the relationship between the DM/EM boundary and the asthenosphere/lithosphere boundary (dashed line) during the evolution of the Rio Grande rift and adjacent regions. Prior to extension and rifting (stage 1), the DM/EM and asthenosphere/lithosphere boundaries coincide, and EM corresponds to lithospheric mantle. This situation presently exists beneath the Great Plains. After extension and rifting have been initiated (stage 2), asthenospheric upwelling and thermal thinning of the lithosphere bring the asthenosphere/lithosphere boundary to the base of the crust. EM has been thinned by extension but is still largely intact. This is the present situation beneath the northern Rio Grande rift. EM now has the physical properties of asthenosphere and begins to convectively mix with the underlying DM/asthenosphere. Alkali basalts still equilibrate within EM. At an advanced stage of extension and rifting (stage 3), extension combined with convective mixing has considerably eroded EM and incorporated it into the DM/asthenosphere, which has now risen to near the base of the crust. Alkali basalts now equilibrate within DM. This stage corresponds to the southern Rio Grande rift and the southern Basin and Range. Alkali basalts from the Colorado Plateau–Basin and Range transition zone equilibrate at the DM/EM boundary, which is at an evolutionary stage between stages 2 and 3.

thenosphere/lithosphere boundary (dashed line in Figure 10) has risen to the base of the crust (Figure 10, stage 2). At this stage the DM/EM boundary is still below the depth of alkali basalt equilibration (45–65 km) and alkali basalts equilibrate within EM. Beneath the rift, EM has asthenospheric physical properties and is able to flow, and the lower parts of EM begin to mix into the small-scale convective flow of DM/asthenosphere. At an advanced stage of rifting (the southern Basin and Range and, by analogy, the southern Rio Grande rift), EM is extensively eroded and incorporated into the DM/asthenosphere by small-scale convection (Figure 10, stage 3). Although a full discussion is beyond the scope of this paper, rifting and erosion of the lithospheric mantle may be a feasible mechanism of introducing enriched mantle components into the convecting upper mantle and could be an important source of mantle heterogeneity.

At an advanced stage of rifting (Figure 10, stage 3), a significant EM component may reside in the uppermost DM/asthenosphere. The small proportion of alkali basalts in the southern Basin and Range that have ε_{Nd} values as low as +5 can be explained by the presence of an EM component in their source, but the larger proportion of alkali basalts with a DM isotopic signature indicates that the DM component is still volumetrically dominant in the uppermost asthenosphere. In contrast, all of the alkali basalts from the Colorado Plateau transition zone have isotopic compositions that indicate a subequal mixture of EM and DM components in their source. Equilibration of these basalts at the depth of the DM/EM boundary (which is probably a gradational boundary several kilometers thick) could account for the consistent presence of both components in their source. This explanation is not unreasonable, since the transition zone lies between the Colorado Plateau, where basalts equilibrate within EM, and the Basin and Range, where basalts equilibrate within DM.

The assumption that compositionally similar alkali basalts equilibrated at similar depths in the mantle allows us to construct a physical model of the DM/EM boundary beneath the rift region (Figure 11). Since alkali basalts from the eastern Colorado Plateau, northern Rio Grande rift, and Great Plains were derived from EM, the DM/EM boundary beneath these areas must lie deeper than the depth of alkali basalt equilibration. Conversely, most basalts from the Basin and Range were derived entirely from DM; hence the DM/EM boundary must be shallower than the depth of alkali basalt equilibration. Basalts from the Colorado Plateau transition zone were derived from a source containing both DM and EM components, most likely the DM/EM boundary.

The configuration of the EM and DM reservoirs beneath the Rio Grande rift region (Figure 11) reflects a recent stage in the evolution of the DM/EM boundary because it is based on the isotopic compositions of basalts <5 m.y. old. In the Lucero volcanic area (Figure 1), alkali basalts that are 7–8 m.y. old (samples 400 and 411) have lower ε_{Nd} values (+3.3 to +4.2) than alkali basalts that are 4 m.y. old and younger (ε_{Nd} of +5.5 to +6.6; samples 328, 384, and 417). These data, considered along with systematic variations in major element compositions through time [*Baldridge et al.*, 1987], suggest that basalts in this area record the rise of the DM/EM boundary between 7 and 4 m.y. ago and the increasing role of DM in the source of the younger basalts at EM is eroded.

Tholeiites: Mantle Sources and Crustal Contamination

Basaltic volcanism in the Rio Grande rift region is characterized by a close spatial and temporal association of olivine tholeiites and alkali basalts (Figure 1 and Table 2). In the Lucero area (Figure 1), for example, a low-alkali tholeiite (sample 324) dated at 0.3 m.y. has $\varepsilon_{Nd} = -0.3$ and $^{87}Sr/^{86}Sr = 0.7064$. This tholeiite erupted only 5 km from the vent of an alkali basalt (sample 328) dated at 0.8 m.y., which has $\varepsilon_{Nd} = +5.5$ and $^{87}Sr/^{86}Sr = 0.7034$. The isotopic compositions of these two basalts encompass nearly the entire range measured in this study (Figure 4) and highlight a fundamental difference between the genesis of alkali basalts and tholeiites in this region. We argue below that the isotopic compositions of Rio Grande rift region tholeiites are generally due to a combination of two factors: derivation from EM and contamination

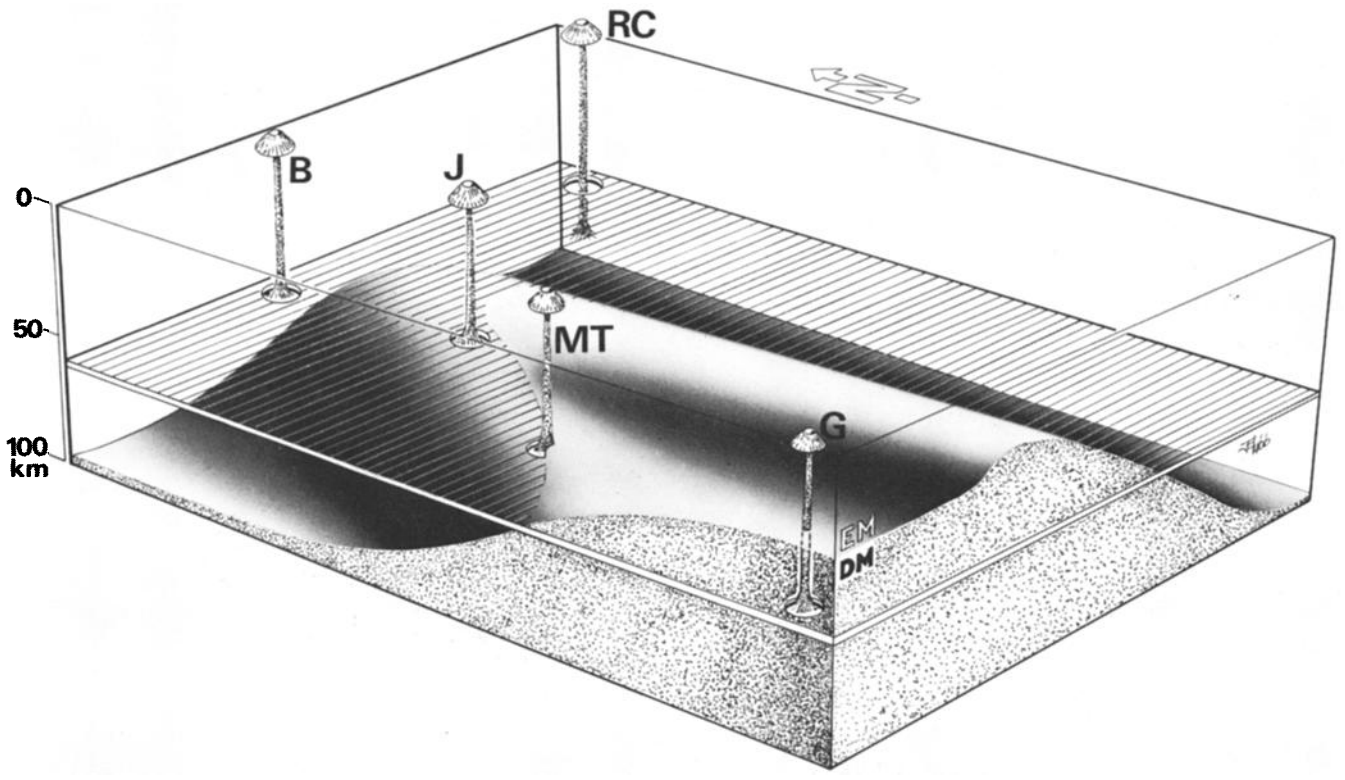

Fig. 11. Block diagram of the Rio Grande rift region, encompassing New Mexico and a portion of eastern Arizona, which illustrates the relationship between mantle source regions and tectonic setting. The shaded surface represents the geochemically defined DM/EM boundary. The ruled plane is a typical depth of alkali basalt equilibration. Note that the crust is not portrayed. Volcanic fields represented area G, Geronimo; MT, Mount Taylor; J, Jemez; B, Brazos; and RC, Raton-Clayton. The mantle source region for a particular alkali basalt depends primarily on the depth to the DM/EM boundary, a function of tectonic setting. Alkali basalts from the southern Basin and Range (Geronimo) are derived from DM. Alkali basalts from the northern Rio Grande rift and adjacent Colorado Plateau and Great Plains (Brazos, Jemez, and Raton-Clayton) are derived from EM. Note that nephelinites from Raton-Clayton, which probably equilibrated at a greater depth than alkali basalts, are still derived from EM due to its thickness beneath the Great Plains. Alkali basalts from the Colorado Plateau transition zone (Mount Taylor) are derived from the DM/EM boundary where it intersects the depth of alkali basalt equilibration. (Illustration by J. Tubb.)

by middle to upper crustal wall rock. In addition, all of the tholeiites have been compositionally modified to some degree by fractional crystallization, as indicated by their low Mg numbers (64.5–59.4).

Mantle source. It is widely accepted, based on may experimental and theoretical studies, that olivine tholeiites generally equilibrate at shallower depths in the mantle (corresponding to a pressure of 7–11 kbar) than alkali olivine basalts (pressures of $\geq$ 11 kbar) [e.g., *Kushiro*, 1968; *Green*, 1971; *Nicholls et al.*, 1971; *DePaolo*, 1979; *Presnall et al.*, 1978, 1979; *Jaques and Green*, 1980; *Fujii and Bougault*, 1983; *Takahashi and Kushiro*, 1983; *Presnall and Hoover*, 1984]. Equilibration of rift region tholeiites at shallower depths than alkali basalts is compatible with the geochemical model of a layered upper mantle presented in the previous section. Thus, if alkali basalts from the Colorado Plateau transition zone equilibrated near the DM/EM boundary as discussed previously, tholeiites from the transition zone probably equilibrated at a depth above the DM/EM boundary within EM. Likewise, since alkali basalts from the northern Rio Grande rift equilibrated within EM, tholeiites from the northern rift (Jemez, Cerros del Rio, Santa Ana Mesa, and Taos Plateau volcanic fields) also must have equilibrated within EM. Tholeiites from the Albuquerque Volcanoes in the central rift have isotopic compositions that are similar to those of alkali basalts from the transition zone, which suggests that they also equilibrated near the DM/EM boundary. If these tholeiites equilibrated at a shallower depth than the alkali basalts, the DM/EM boundary must be at a shallower depth beneath the central rift axis, as is the asthenosphere/lithosphere boundary [e.g., *Olsen et al.*, 1979]. With the exception of tholeiites from the Albuquerque Volcanoes, we conclude that all of the tholeiites considered in this paper equilibrated within EM (Figure 12).

EM-derived tholeiites from this study do not have the same isotopic compositions as EM-derived alkali basalts but instead always have higher $^{87}Sr/^{86}Sr$ (Figure 4). In a detailed Sr isotopic study of the Cerros del Rio field in the northern rift, *Crowley* [1984] found the same systematic shift in $^{87}Sr/^{86}Sr$. Twelve alkali basalts have $^{87}Sr/^{86}Sr$ ranging from 0.7039 to 0.7042 (EM source), while four tholeiites have $^{87}Sr/^{86}Sr$ ranging from 0.7047 to 0.7049. These results agree with our measurements of an alkali basalt and tholeiite (samples 61 and 87, respectively) from the Cerros del Rio field. In general, therefore, we can be fairly certain that tholeiites from the rift region have systematically higher $^{87}Sr/^{86}Sr$ compared to alkali basalts, even when both have equilibrated within EM.

The systematically higher $^{87}Sr/^{86}Sr$ of the tholeiites could simply reflect a heterogeneous EM source. We will argue in a later section that the EM source is in fact heterogeneous, but we do not think that this heterogeneity can account for the

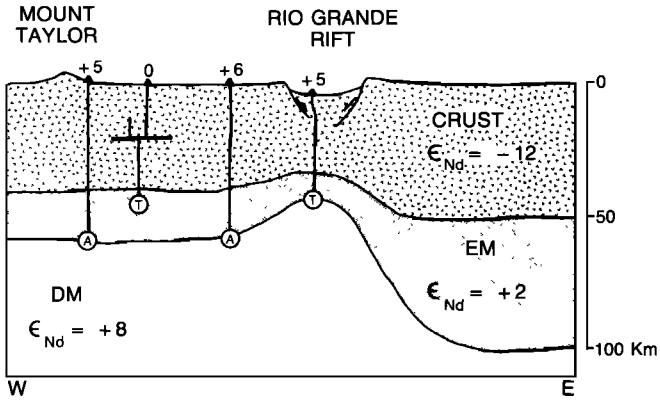

Fig. 12. Schematic cross section showing mantle structure and its relation to basalt genesis beneath the Colorado Plateau–Basin and Range transition zone and the central Rio Grande rift. The ε_{Nd} of EM and DM represent values of derived melts and imply nothing about mantle homogeneity. Numbers on the earth's surface are ε_{Nd} values of the erupted basalts. Alkali basalts (A) from the transition zone equilibrate at the DM/EM boundary and ascend without crustal interaction to erupt with ε_{Nd} values that reflect the relative proportions of DM and EM components incorporated in the mantle source region. Tholeiites (T) from the transition zone equilibrate within EM but, because of a longer crustal residence time, are contaminated by minor amounts of middle to upper crustal wall rock and erupt with ε_{Nd} values that are shifted slightly toward crustal ε_{Nd} values. Tholeiites from the central Rio Grande rift are derived from the elevated DM/EM boundary and ascend through the crust with little crustal interaction, perhaps due to the more pronounced deformation within the rift axis, as evidence by fault displacements of several kilometers versus tens to hundreds of meters in the transition zone [*Olsen et al.*, 1987].

higher $^{87}Sr/^{86}Sr$ of the tholeiites. If a plum pudding model accounts for EM heterogeneity and it is heterogeneous on a small scale, tholeiites would have to preferentially tap the enriched components in the source compared to the alkali basalts. If a small-scale heterogeneous source is able to produce isotopic differences between tholeiites and alkali basalts, we would expect that the alkali basalts, representing the smaller degree of partial melting, would preferentially incorporate the less refractory, more enriched components, but this is exactly the opposite of what we observe. If the isotopic differences reflect heterogeneity on a larger scale (i.e., kilometers), we can conceive of no mechanism that would cause tholeiites to always tap the more enriched regions of the mantle. Another possibility, which cannot be evaluated using the available data, is that the EM source is isotopically zoned with the upper portion (tholeiite source) having higher $^{87}Sr/^{86}Sr$.

Crustal contamination. We propose that the higher $^{87}Sr/^{86}Sr$ of the tholeiites compared to EM-derived alkali basalts is not due to a heterogeneous mantle source but is instead due to interaction with high-$^{87}Sr/^{86}Sr$ wall rock of the middle to upper crust. Crustal contamination can be evaluated quite rigorously for tholeiites of the rift region and can reasonably account for all of their geochemical and isotopic characteristics.

The nearly horizontal trend defined by these tholeiites (a shift to higher $^{87}Sr/^{86}Sr$ with only a small shift to lower ε_{Nd}; Figure 9) indicates that the contaminant has high $^{87}Sr/^{86}Sr$. *DePaolo and Wasserburg* [1979*b*] and *DePaolo* [1981*a*] presented a generalized model for the Nd and Sr isotopic composition of Precambrian upper and lower crust. According to this model, granulite-facies lower crust has relatively low $^{87}Sr/^{86}Sr$ as a result of Rb depletion during high-grade (granulite facies) metamorphism, while upper crustal rocks have high $^{87}Sr/^{86}Sr$. Sm-Nd systematics are relatively unaffected by high-grade metamorphism, and Nd isotopic compositions are thus approximately the same in both the upper and lower crust.

Isotopic data from the Rio Grande rift region indicate that the above model can be applied to the upper and lower crust of the rift region. For example, nearly all measured Precambrian granitic (and thus presumably upper crustal) rocks of New Mexico have $^{87}Sr/^{86}Sr$ greater than 0.72 (95% of 175 samples, Figure 13). In contrast, granulites (presumably representing lower crust) from the Precambrian of Colorado, part of the same crustal terrane as is present in northern New Mexico, have $^{87}Sr/^{86}Sr$ less than 0.71 [*DePaolo*, 1981*a*, *b*].

The best evidence that the lower crust beneath the rift region is characterized by low $^{87}Sr/^{86}Sr$ comes from crustally contaminated volcanic rocks of the Taos Plateau and Jemez volcanic fields. Because contamination of magmas involves a relatively large "sampling" of crust, isotopic trends that result from contamination can be considered to reflect the "average" properties of that crust. In contrast, characteristics of the lower crust inferred from studies of lower crustal xenoliths may only reflect the characteristics of a small sample population and not the bulk characteristics of a heterogeneous region. Lead isotopic compositions of basalts, andesites, and dacites of the Taos Plateau become systematically less radiogenic with increasing SiO_2 content [*Dungan et al.*, 1986], strongly indicating progressive contamination of magmas by old, uranium-depleted wall rock. Uranium depletion is characteristic of granulite-facies lower crust [e.g., *DePaolo et al.*, 1982; *Rudnick et al.*, 1985]. The Taos Plateau lead data are coupled to Nd and Sr isotopic data which define a vertical trend of decreasing ε_{Nd} with relatively little shift to higher $^{87}Sr/^{86}Sr$ [*Williams*, 1984]. This trend, which is fundamentally different from the nearly horizontal trend defined by tholeiitic

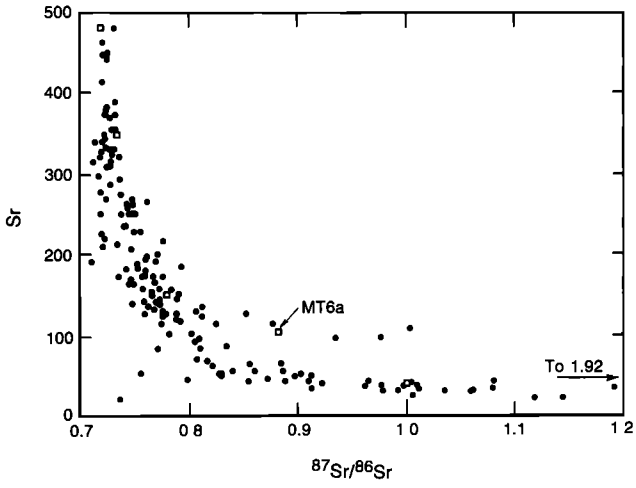

Fig. 13. Sr versus measured $^{87}Sr/^{86}Sr$ for New Mexico Precambrian rocks. Rock types include granite, granodiorite, quartz monzonite, quartz diorite, granitic gneiss, schist, and felsic metavolcanic rocks. Data sources are *Mukhopadhyay et al.* [1975], *Taggart and Brookins* [1975], *White* [1978], *Wobus and Hedge* [1980], *Brookins et al.* [1980, 1985], *Brookins and Majumdar* [1982], and *Brookins and Laughlin* [1983]. Model values (open squares) used in AFC calculations include a value not shown at $^{87}Sr/^{86}Sr$ = 1.5 and Sr = 25 ppm. MT6a is a granite xenolith from the Mount Taylor volcanic field. Five samples not shown have $^{87}Sr/^{86}Sr$ ranging from 1.25 to 1.92 with Sr = 51 to 10 ppm.

basalts of this study, indicates contamination by low-$^{87}Sr/^{86}Sr$ wall rock. In light of the lead data, this low-$^{87}Sr/^{86}Sr$ wall rock is best interpreted as residing in the lower crust. Nd and Sr isotopic data from basalts, andesites, and dacites of the Jemez volcanic field [*Loeffler and Futa*, 1985] also display a vertical Nd-Sr trend compatible with contamination by low-$^{87}Sr/^{86}Sr$ lower crustal wall rock. Thus the lower crust beneath the Rio Grande rift region appears to be largely composed of granulite-facies rock characterized by low $^{87}Sr/^{86}Sr$, Rb/Sr, and U/Pb. Contamination by lower crust with these characteristics could not produce the isotopic array displayed by the tholeiites of this study.

All of the tholeiites that we have studied represent some degree of fractional crystallization from primary melts, as indicated by their low Mg numbers (64.5–59.4). If these tholeiites are crustally contaminated, we assume that fractional crystallization accompanied crustal contamination and have used the assimilation/fractional crystallization (AFC) equations of *DePaolo* [1981*c*] to model their evolution. To model quantitatively the AFC evolution of a magma, it is necessary to know the magma's fractionation history and the geochemical characteristics of the assimilated wall rock. These parameters can be estimated with some confidence for tholeiites and for the upper crust in the rift region.

Only a few Nd isotopic measurements have been made for upper crustal granitic rocks in this region. These include 1.7-b.y.-old granodiorites from northern New Mexico and Colorado [*DePaolo*, 1981*b*] with $\varepsilon_{Nd} = -11.2$ to -13.3 and Nd = 16 to 42 ppm; a 1.4-b.y.-old anorogenic granite from the central Rio Grande rift [*Nelson and DePaolo*, 1985] with $\varepsilon_{Nd} = -12.9$ and Nd = 65 ppm; and a granite xenolith (MT6a) from the Mount Taylor volcanic field (F. V. Perry, unpublished data, 1987) with $\varepsilon_{Nd} = -15.0$ and Nd = 56 ppm. The Nd isotopic composition of upper crustal granitic rocks from this region can also be estimated from their age and Sm/Nd ratios, a ratio which is fairly constant for most crustal rocks. Assuming a range in $f_{SM/Nd}$ (the Sm/Nd enrichment factor) of -0.35 to -0.45 for upper crust [*DePaolo and Wasserburg*, 1979*b*] and an age of 1.7 b.y., ε_{Nd} of the upper crust is calculated to range from about -11 to -15, using the depleted mantle model of *DePaolo* [1981*b*]. This calculated range of values coincides with the measured range; $\varepsilon_{Nd} = -12$ and Nd = 30 ppm are thus reasonable model values for the upper crustal contaminant. We have also used the Mount Taylor granite xenolith as a contaminant since it is a direct sample of basement beneath the Colorado Plateau transition zone, and it extends the range of our model values to lower ε_{Nd} and higher Nd.

In contrast to Nd, the Sr concentrations and isotopic compositions of upper crustal basement rocks in New Mexico encompass a large range of values. However, because $^{87}Sr/^{86}Sr$ and Sr concentrations of upper crustal rocks are inversely correlated (Figure 13), the exact values chosen are not critical. This is because the isotopic shifts produced in a magma by contamination are dependent on the product of the isotopic composition and the elemental concentration of the contaminant [*DePaolo*, 1985]. To demonstrate this, several crustal values were used in our model, chosen to cover a range of isotopic values and concentrations (Figure 13).

To model the fractionation history of the Colorado Plateau tholeiites, all of which contain olivine and plagioclase as phenocryst phases, we used the program EQUIL [*Nielsen and Dungan*, 1983; *Nielsen*, 1985], which simulates low-pressure fractionation in mafic systems. For a starting composition we chose an olivine tholeiite from *Takahashi and Kushiro* [1983; Table 3, KRB, 10.5 kbar], which is very similar in major element composition to tholeiites of the Colorado Plateau transition zone but has a primitive Mg number of 70. This model indicates that the transition zone tholeiites represent an F value (fraction of residual magma) of 0.9–0.8 (constrained to correspond to Mg numbers of 60–65) with olivine + plagioclase + trace spinel being the fractionating phases. The cumulative fraction of plagioclase removed in the fractionating assemblage is 0.27 for $F = 0.9$, increasing to 0.48 for $F = 0.8$. These proportions are reasonable because olivine was probably the liquidus phase and the dominant fractionating phase during the early stages of fractionation. Using this approximate fractionating mineral assemblage and appropriate partition coefficients for Sr and Nd [*Drake and Weill*, 1975; *Hanson*, 1980] gives $D_{Sr} = 0.5$ and $D_{Nd} = 0.1$, where D is the bulk crystal/liquid partition coefficient. These D values can be taken as constant over the small range of crystallization considered.

We made no attempt in our AFC calculations to model the evolution of individual tholeiites, only the general trend that the tholeiites define. Each tholeiite undoubtedly evolved along a unique AFC path, but the coherent trend indicates that these paths were grossly similar. Five AFC models were calculated using a bulk crustal contaminant composition of $\varepsilon_{Nd} = -12$, Nd = 30 ppm, and a range of $^{87}Sr/^{86}Sr$ and Sr values (Figure 13). In addition, a granite xenolith from Mount Taylor (MT6a) was used as a crustal contaminant. All of these models produce very similar results (Figure 9). This illustrates that because the upper crust in this region has a relatively uniform Nd isotopic composition and Sr isotopic compositions that vary systematically with Sr concentration, nearly all upper crustal contaminants (or combinations of contaminants) will produce an AFC curve consistent with the tholeiite trend. This result is also compatible with a physical model in which tholeiites rising through the crust are exposed to a variety of wall rock compositions.

The AFC curve shown in Figure 9 for the Colorado Plateau tholeiites illustrates several features common to all of the calculated models. First, the F values shown are slightly higher than the F values estimated from simple fractionation because they take into account the mass added to the magma by assimilation. The F value for simple fractionation is always a minimum value, but the two cases converge for large F values or small values of r (assimilation rate/crystal fractionation rate). Second, if the F value, composition of the contaminant, and initial composition of the magma (see Figure 9 caption) can be estimated, values of r can be determined by trial and error (varying r until the F values are appropriate) or by using equation (4) of *DePaolo* [1985], which relates the rate of change of the isotopic composition (in terms of F) to r. These calculations show that values for the parameter r of between 0.2 and 0.3 were likely during the evolution of the tholeiites. From these values, the ratio of the mass assimilated to the original mass of magma, $M_a/M_m{}^0$ [*Farmer and DePaolo*, 1983], can be calculated and fall in the range of 0.03–0.08 in all the models considered. Such low values of $M_a/M_m{}^0$ would not generally be noticeable in the major element chemistry, but elements such as Rb and K appear to be sensitive indicators of contamination by Rb-rich (upper crustal) wall rock (Figure 14).

Compared to tholeiites from the Colorado Plateau transi-

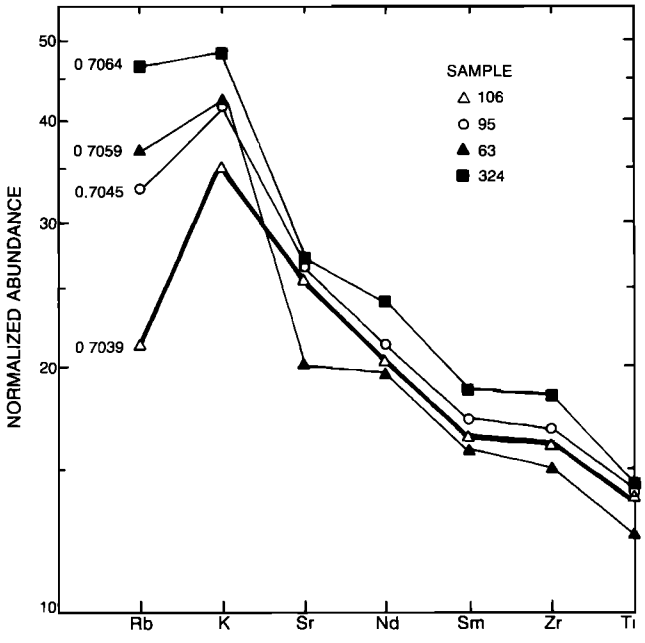

Fig. 14. Normalized trace element abundances [after *Thompson et al.*, 1982] for selected low-alkali tholeiites. Rb and K show the largest variations among these tholeiites, and their abundances correlate with degree of crustal contamination as indicated by $^{87}Sr/^{86}Sr$ values (shown next to Rb values). Samples 106 and 95, both from the Albuquerque Volcanoes, are assumed to be derived from the same mantle source, indicating that the Rb and K variations are due to small amounts of crustal contamination and not differences in mantle source regions.

tion zone, tholeiites from the Rio Grande rift have lower $^{87}Sr/^{86}Sr$ at a similar degree of chemical evolution. Tholeiites from the northern rift are from volcanic fields peripheral to the Jemez volcanic field where Nd and Sr isotopic data [*Loeffler and Futa*, 1985] indicate contamination by low-$^{87}Sr/^{86}Sr$ lower crustal wall rock. It is possible then that the relative lack of $^{87}Sr/^{86}Sr$ enrichment in the northern rift tholeiites is due to a larger component of lower crustal contamination. Another possibility is that these rift tholeiites are contaminated by upper crustal wall rock, but to a lesser degree than Colorado Plateau tholeiites (Figure 12). This possibility was modeled for the Albuquerque Volcanoes (Figure 9). Sample 106 is not (or is only minimally) crustally contaminated based on its isotopic composition and, significantly, has the lowest Rb content (7.4 ppm) of any of the tholeiites in this study. Using the isotopic and trace element composition of sample 106 as a parental composition and a likely degree of crystallization based on Mg number, sample 95 is modeled as having undergone a small amount of upper crustal contamination. The parameter r is smaller than in the case of the Colorado Plateau tholeiites (0.15 versus 0.3) and $M_a/M_m{}^0$ is between 0.01 and 0.02. Despite this small amount of contamination, the Rb content of sample 95 (11.5 ppm) is 50% higher than that of sample 106, attesting to the sensitivity of Rb as an indicator of upper crustal contamination.

Crustal Contamination: Relation to Magma Composition and Crustal Structure

There is no evidence that the alkali basalts of this study, which are typical of most rift region alkali basalts, have been crustally contaminated. In contrast, the geochemistry and isotopic compositions of tholeiites can be well accounted for by a model of fractional crystallization combined with small amounts of crustal contamination. We hypothesize that this difference reflects small but significant differences in the physical properties of alkalic and tholeiitic magmas, properties which control their relative ascent rates through the crust and thus their opportunity to interact with crustal wall rock.

A first-order indication of relative ascent rate is the presence or absence of mantle xenoliths, which are often found in rift region alkali basalts but have never been observed in rift region tholeiites. We accept the implication that tholeiite ascent rates are insufficient to entrain dense mantle xenoliths. Factors which influence the ascent rate of a magma include volatile content, density, and viscosity. Alkali basalts in the rift region generally erupt to form cinder cones, while tholeiites typically erupt from fissure systems or shield cones [e.g., *Baldridge et al.*, 1987], indicating that alkaline magmas have a higher volatile content at the time of eruption. High volatile contents play an important role in the rapid ascent of alkaline magmas, mainly by controlling the initial ascent velocity via a crack propagation mechanism [*Spera*, 1984]. Higher volatile content also decreases magma viscosity and density, further enhancing magma ascent. *Kushiro* [1982] determined experimentally that at pressures of 7–15 kbar, alkali basalts are inherently less dense than tholeiites and attributed this to the relatively large partial molar volumes of alkalis in silicate melts.

Crustal properties also undoubtedly play a key role in controlling the ascent of magmas. *Olsen et al.* [1987] emphasized the dominance of horizontal structures within the middle and upper crust of the Rio Grande rift region. A prominent feature of this horizontally stratified crust is a well-defined Conrad discontinuity at about 20 km depth, which corresponds to a density interface within the crust [*Toppozada and Sanford*, 1976; *Olsen et al.*, 1979]. This level of the middle crust was probably extended by discontinuous ductile flow resutling in subhorizontal, lensoidal "megaboudins" of contrasting physical properties. Slowly ascending tholeiitic magmas would have difficulty traversing such a horizontally stratified density interface within the crust. They would likely pause to form sill-like magma bodies such as the Socorro magma chamber found at midcrustal depths in the south central Rio Grande rift [*Rinehart et al.*, 1979]. Sill-like magma chambers would have large surface area/volume ratios and would be favorable sites for crustal contamination to occur.

If all types of volcanic rocks (excluding rhyolites) from the Rio Grande rift region are considered, significant differences are apparent concerning the depth of crustal contamination (upper versus lower crust). Different depths of contamination can be related to differences in the thermal and structural characteristics of crust within the rift compared to those of crust outside of the rift.

Tholeiites from the Colorado Plateau–Basin and Range transition zone were contaminated by middle to upper crustal wall rock, as discussed previously. The Nd and Sr isotopic compositions of latites and quartz latites from the Mount Taylor volcanic field, which is within the transition zone (Figure 1), also suggest contamination by predominantly upper crustal wall rock [*Perry et al.*, 1983; F. V. Perry, unpublished data, 1987]. In contrast, volcanic rocks showing evidence of lower crustal contamination occur within the rift and are associated with large-volume, long-lived volcanic fields (specifically, the Jemez and Taos Plateau volcanic fields, the most voluminous fields in the Rio Grande rift). For example, several andesites and dacites from the Taos Plateau have

$\varepsilon_{Nd} < -12$ and $^{87}Sr/^{86}Sr < 0.706$ [*Williams*, 1984], indicating a very large component of lower crustal melt. Alkali basalts from the Taos Plateau (discussed below) probably also interacted with lower crust, in contrast to alkali basalts elsewhere in the rift region, suggesting that possibly no magmas could ascend through the crust in this area without undergoing some lower crustal interaction. The lower crust beneath the Taos Plateau must have been unusually hot, not only because of higher background temperatures in the lower crust of the rift compared to lower crust beneath the rift flanks [e.g., *Olsen et al.*, 1987] but also because of local heat input associated with the large volumes of volcanic rocks that were erupted. Both of these conditions may have to exist concurrently in order for significant lower crustal contamination to occur. Note that tholeiites from the Albuquerque Volcanoes, a short-lived volcanic field of small volume within the Rio Grande rift, do not appear to have interacted with lower crustal wall rock (Figure 9). High temperatures within the lower crust of the rift could promote incorporation of lower crustal materials into magmas because (1) the hot lower crust has a slightly lower density, which would tend to slow magma transit through it, and (2) wall rock is closer to its melting point and can therefore be more easily melted and incorporated into the rising magmas. Once magmas passed into the brittlely extended upper crust of the fit, access to deeper, more throughgoing fracture systems (compared to fractures on the rift flanks) might result in minimal wall rock interaction before eruption.

Alkali basalts of the Taos Plateau probably interacted with lower crustal wall rock. These alkali basalts do not carry mantle xenoliths and are compositionally evolved, with SiO_2 ranging from 50 to 53 wt % and Mg numbers <58 [*Lipman and Mehnert*, 1975, 1979*a*; *Basaltic Volcanism Study Project*, 1981; *Dungan et al.*, 1984]. Their major element and isotopic compositions are distinct from most other alkali basalts in the rift region and are compatible with a petrogenesis involving lower crustal interaction. We have calculated a generalized AFC curve for tholeiites and alkali basalts of the Taos Plateau (Figure 9) that uses a likely lower crustal composition as a contaminant. A major difference between our model of basalt contamination and that of *Williams* [1983, 1984] is the choice of a mantle end-member. Williams assumed that the source region beneath the Taos Plateau was asthenosphere that gave rise to MORB-like parental melts (i.e., $\varepsilon_{Nd} = +11$ and $^{87}Sr/^{86}Sr = 0.7025$), despite the fact that no basalts in the volcanic field are known to have $\varepsilon_{Nd} > 0$. We suggest that the source of Taos Plateau basalts was EM that had been thermally converted to asthenosphere, as indicated by the isotopic compositions of uncontaminated alkali basalts from other areas of the northern rift and the adjacent Colorado Plateau and Great Plains (Table 3 and Figure 7).

Nature of the Subcontinental Lithospheric Mantle

Characterization of EM/lithosphere beneath the Rio Grande rift region encounters an apparent paradox. Evidence for heterogeneity in the EM source beneath the Rio Grande rift region comes from studies of lithospheric spinel lherzolite xenoliths entrained in asthenosphere-derived alkali basalts [*Jagoutz et al.*, 1980; *Menzies et al.*, 1985; *Zindler and Jagoutz*, 1987]. Clinopyroxenes, representing the major reservoirs of Nd and Sr in these xenoliths, have isotopic compositions ranging from MORB-like values ($\varepsilon_{Nd} = +13$) to values near $\varepsilon_{Nd} = 0$ (Figure 15). These data highlight the extreme isotopic diversity to be found within the EM source. EM-derived alkali

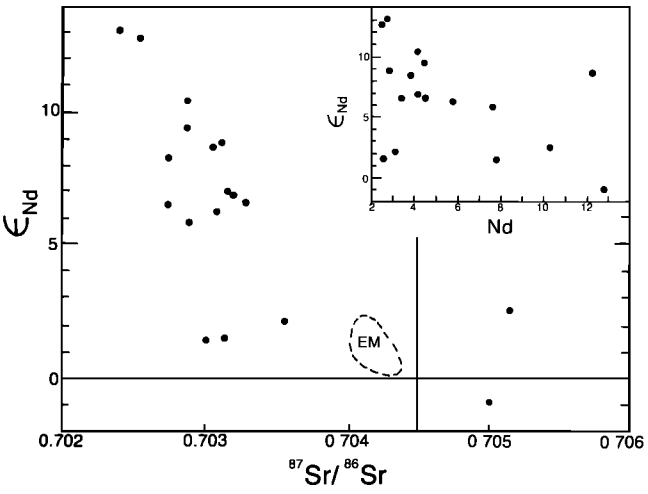

Fig. 15. Measured ε_{Nd} versus $^{87}Sr/^{86}Sr$ for clinopyroxenes in spinel lherzolite xenoliths from the San Carlos and Geronimo volcanic fields, Arizona, and Kilbourne Hole, New Mexico [*Jagoutz et al.*, 1980; *Menzies et al.*, 1985; *Zindler and Jagoutz*, 1987]. "EM" is the field for EM-derived alkali basalts (Figure 9). The ε_{Nd} versus Nd for clinopyroxenes (inset) shows that the most isotopically "enriched" (lowest ε_{Nd}) clinopyroxenes tend to be most enriched in Nd.

basalts, however, even though erupted several hundred kilometers apart (Figure 7), display a very limited range of isotopic compositions (Figure 15), suggesting a homogeneous EM source. This paradox can be resolved with a plum pudding model analogous to that proposed earlier for DM/asthenosphere. We think that the bulk of EM is composed of incompatible-element-depleted lherzolite that represents convecting upper mantle converted to lithosphere at the time of crustal formation and stabilization of the lithosphere 1.7 b.y. ago. Within the depleted lherzolite matrix occur numerous small volumes of incompatible-element-enriched lherzolite or magmatic intrusions. Some of these enriched heterogeneities were present prior to lithosphere stabilization, others were created during and subsequent to lithosphere stabilization by migrating melts and associated fluid phases [e.g., *Spera*, 1984; *Wilshire*, 1984; *Menzies et al.*, 1985].

We assume that the isotopic compositions of clinopyroxenes from spinel lherzolites represent the isotopic diversity within EM beneath the Rio Grande rift region. Melting of heterogeneous EM thus involves a combination of enriched and depleted components. Probably only the least refractory and most enriched components in any volume of mantle would be significantly involved in a melting event. This is compatible with field data showing that basalt fields of the Rio Grande rift region typically include a range of compositions and are of small volume (several to a few tens of cubic kilometers of erupted material, accumulated after many separate eruptions). These relationships imply a heat source that produces only isolated instances of local melting [*Olsen et al.*, 1987]. Under these conditions, the enriched and less refractory components would dominate the isotopic compositions of melts, since they contribute more to the melt and tend to have higher incompatible element concentrations (Figure 15, inset). The isotopic compositions of EM-derived basalts (Figure 15) would thus be weighted toward the more enriched, less refractory (and less abundant) components in the source and would not be representative of the "bulk" isotopic composition of

EM. The more "enriched" isotopic signature of heterogeneous EM compared to heterogeneous DM can be accounted for by differences in the nature of their enriched heterogeneities. Heterogeneities in EM are probably on the average more isotopically "enriched" because of their long-term isolation from major melting (depletion) events and upper mantle convection. Just as for DM, the isotopic homogeneity of EM-derived basalts implies that EM, while heterogeneous on a small scale, is "homogeneous" on a regional scale.

Finally, the isotopic composition of incompatible-element-enriched components in the EM/lithosphere is partly a function of their age. A plausible mechanisms for the enrichment of lithosphere involves a large flux of magma and fluids through newly stabilized lithosphere at the time of local crust formation. Thus each segment of Precambrian continental crust in the western United States [see *Nelson and DePaolo*, 1985] is underlain by lithospheric mantle of equivalent age possessing isotopic characteristics which reflect that age. For example, volcanic rocks from the Archean craton of Wyoming, Montana, and Idaho have lower ε_{Nd} values compared to Rio Grande rift region basalts, consistent with derivation from a lithospheric mantle source that is considerably older (2.7 b.y. old versus 1.7 b.y. old) than that beneath the rift region, but not necessarily different in the degree of incompatible-element enrichment.

The isotopic compositions of uncontaminated volcanic rocks from the Archean craton correlate with composition, a relationship we do not see in the rift region. Mafic ultrapotassic volcanic rocks form Leucite Hills, Wyoming [*Vollmer et al.*, 1984] and Smoky Butte, Montana [*Fraser et al.*, 1986] have low ε_{Nd} values (-10 to -26), while olivine tholeiites from the Snake River Plain show a more restricted range of ε_{Nd} values of -3 to -6 [*Menzies et al.*, 1983]. All of these volcanic rocks have a similar $^{87}Sr/^{86}Sr$. This relationship is compatible with a plum pudding model for the Archean lithosphere. The ultrapotassic rocks could represent extremely small amounts of partial melt that sampled only the least refractory, LREE-enriched component within the Archean lithosphere (a small fraction of melting from the previously unmelted "plums"). Snake River Plain olivine tholeiites, which are both voluminous and homogeneous in composition (apparently due to a long-lived and major heat source), represent melting of a much greater volume of mantle, and they presumably sampled a greater proportion of refractory, LREE-depleted lherzolite. Alternatively, since ultrapotassic rocks are probably derived from a much greater depth than olivine tholeiites, the Archean lithosphere may be zoned, becoming more LREE enriched (greater magma and fluid flux?) with depth [*Farmer*, 1987].

In the Rio Grande rift region, stabilization of the lithospheric mantle was more recent. This lithosphere is therefore characterized by higher ε_{Nd} values than Archean lithosphere. Thus this model involving the structure and age of subcontinental lithospheric mantle is compatible with the observed range in isotopic values of lithosphere-derived basalts throughout the western United States.

SUMMARY

1. Alkali basalts from the Rio Grande rift region are generally unaffected by crustal contamination and were derived from two distinct mantle sources which we characterize as "depleted" mantle (DM) and "enriched" mantle (EM). Alkali basalts from areas of pronounced lithospheric extension (southern Basin and Range and southern Rio Grande rift) equilibrated within DM, which corresponds to upwelled asthenosphere. Alkali basalts from areas of relatively less extension (northern Rio Grande rift, eastern Colorado Plateau and Great Plains) equilibrated witin EM. Alkali basalts from the Colorado Plateau–Basin and Range transition zone were derived from a mixed zone at the DM/EM boundary. EM corresponds to lithospheric mantle prior to extension and disruption of the lithosphere. At an intermediate stage of extension, the lithosphere is thermally converted to asthenosphere, but EM remains physically intact. At an advanced stage of extension, EM is extensively eroded by convective mixing and is replaced by DM.

2. Tholeiites, which equilibrate at a shallower depth than alkali basalts, generally equilibrated within EM. The tholeiites that we have studied have higher $^{87}Sr/^{86}Sr$ compared to EM-derived alkali basalts, which can be accounted for by assimilation of small amounts ($<10\%$) of middle to upper crustal wall rock. This amount of assimilation is not measurably reflected in the major element chemistry but can be detected by higher concentrations of Rb and, to a lesser extent, K. Crustal contamination of tholeiites may be favored relative to alkali basalts because of their slower ascent rate through the crust, which is partly a function of volatile content and magma density.

3. Volcanic rocks from the most voluminous volcanic fields within the Rio Grande rift (Jemez and Taos Plateau volcanic fields) are contaminated primarily by lower crustal wall rock. Sites of more voluminous volcanism may locally enhance thermal input into the lower crust, and it may be that this additional thermal input into an already hot lower crust is necessary for significant lower crustal contamination to occur.

4. The isotopic compositions of EM- and DM-derived basalts can be accounted for by a "plum pudding" model of the mantle in which small-scale, trace element and isotopically "enriched" heterogeneities are embedded in a "depleted" and more refractory lherzolite matrix. Although both DM and EM are heterogeneous on a small scale, they are "homogeneous" on a regional scale. The more "enriched" isotopic signature of EM relative to DM reflects the age of the lithospheric mantle beneath this region and its long-term isolation from the underlying, convecting asthenosphere. Regional extension and rifting are rapidly bringing isolation of lithospheric mantle to an end.

APPENDIX: SAMPLE LOCATIONS

Sample 7. Lower flow, southeast edge of La Jara Mesa. San Mateo 7.5-minute quadrangle (quad.) 107°41′13″W, 35°15′12″N.

Sample 22. Flow extending west from cinder cone on northeast corner of Horace Mesa. Lobo Springs, 7.5-minute quad. 107°39′28″W, 35°13′04″N.

Sample 9. Lowest flow on northeast side of Horace Mesa at Big Spring. Lobo Springs 7.5-minute quad. 107°40′00″W, 35°11′43″N.

Sample 31. Capping flow from exposure in upper Rinconada, Canyon, southeastern flank of Mount Taylor. Lobo Springs 7.5-minute quad. 107°38′20″W, 35°12′14″N.

Sample 328. Flow extending northwest from Volcano Hill. Cerro Verde 7.5-minute quad. 107°19′22″W, 34°49′07″N.

Sample 384. Middle flow in canyon on west side of Tres Hermanos Mesa. Table Mountain 7.5-minute quad. 107°33′03″W, 34°29′37″N.

Sample 417. East side of plug, westernmost Tres Hermanos Peaks. Table Mountain 7.5-minute quad. 107°33'03"W, 34°27'29"N.

Sample 400. Third flow from top of exposure on northeast edge of Chicken Mountain. Chicken Mountain 7.5-minute quad. 107°16'47"W, 34°39'47"N.

Sample 411. Second flow above base of exposure on southeast edge of Mesa Gallina. Mesa Aparejo 15-minute quad. 107°13'45"W, 34°43'02"N.

Sample 89. North side of Cerro de Guadalupe plug, Puerco Necks. Guadalupe 7.5-minute quad. 107°08'20"W, 35°33'59"N.

Sample 142. Upper flow, approximately 100 m south of Bandera Crater breach. Ice Caves 7.5-minute quad. 108°05'07"W, 34°59'48"N.

Sample 425. Flow extending from small cinder cone 4 km southeast of Red Hill. Red Hill 7.5-minute quad. 108°49'10"W, 34°12'37"N.

Sample 143. Flow on east side of Cat Hills. Dalies 7.5-minute quad. 106°48'56"W, 34°52'28"N. Additional data from *Baldridge et al.* [1982].

Sample 61. Capping flow on rim of White Rock Canyon. Cochiti Dam 7.5-minute quad. 106°18'23"W, 35°39'35"N.

Sample 63. Flow east of Laguna. Mesita 7.5-minute quad. 107°20'33"W, 35°02'34"N.

Sample AWL-40-70. Laguna flow of *Nichols* [1946]. Lies beneath the McCartys flow. Grants SE 7.5-minute quad. 107°46'39"W, 35°05'28"N. Collected by A. W. Laughlin.

Sample 324. Distal end of flow originating at Cerro Verde. From roadcut on Highway 6. South Garcia 15-minute quad. 107°03'05"W, 34°50'18"N.

Sample 329. Capping flow on east edge of Mesa del Oro. Chicken Mountain 7.5-minute quad. 107°22'14"W, 34°41'26"N.

Sample 95. Lower flow from exposure on south side of Albuquerque Volcanoes. La Mesita Negra SE 7.5-minute quad. 106°45'38"W, 35°06'45"N.

Sample 106. Lower flow from exposure on east side of Albuquerque Volcanoes. Los Griegos 7.5-minute quad. 106°43'22"W, 35°09'52"N.

Sample 65. Bomb from quarry in cinder cone on Santa Ana Mesa. San Felipe Pueblo 7.5-minute quad. 106°29'26"W, 35°29'48"N.

Sample 87. Flow in Ancho Canyon. White Rock 7.5-minute quad. 106°14'38"W, 35°46'52"N.

Acknowledgments. This work was supported by the Institute of Geophysics and Planetary Physics of the University of California (Los Alamos Branch), the Office of Basic Energy Sciences of the U.S. Department of Energy, and by National Science Foundation grant EAR84-15143 (D.J.D). We thank D. Curtis and G. Lang Farmer for their generous help in acquiring the isotopic measurements at Los Alamos. G. Luedemann provided the X ray fluorescence analyses. J. Tubb, A. Kron, A. Garcia, and J. Archuleta drafted the figures. A. W. Laughlin provided sample AWL-40-70. B. Crowe, D. Curtis, G. Lang Farmer, J. N. Gardner, and K. H. Olsen were sources of valuable discussion and criticism. We appreciate critical reviews of an earlier version of this paper by B. Crowe, D. Curtis, A. W. Laughlin, K. H. Olsen, and D. Vaniman and journal reviews by S. R. Hart and R. E. Zartman, all of which resulted in substantial improvement of the original manuscript.

REFERENCES

Aldrich, M. J., Jr., and A. W. Laughlin, A model for the tectonic development of the southeastern Colorado Plateau boundary, *J. Geophys. Res.*, *89*, 10,207–10,218, 1984.

Allègre, C. J., B. Dupré, B. Lambret, and P. Richard, The subcontinental versus suboceanic debate, I, Pb-Nd-Sr isotopes in primary alkali basalts from a shield area: The Ahaggar volcanic suite, *Earth Planet. Sci. Lett.*, *52*, 85–92, 1981.

Allègre, C. J., B. Dupré, P. Richard, and D. Rousseau, Subcontinental versus suboceanic mantle, II, Nd-Sr-Pb isotopic comparison of continental tholeiites with mid-ocean ridge tholeiites, and the structure of the continental lithosphere, *Earth Planet. Sci. Lett.*, *57*, 25–34, 1982.

Allègre, C. J., B. Hamelin, and B. Dupré, Statistical analysis of isotopic ratios in MORB: The mantle blob cluster model and the convective regime of the mantle, *Earth Planet. Sci. Lett.*, *71*, 71–84, 1984.

Ander, M. E., Geophysical study of the crust and upper mantle beneath the central Rio Grande rift and adjacent Great Plains and Colorado Plateau, *Los Alamos Natl. Lab. Rep. LA-8676-T*, 218 pp., 1981.

Aoki, K., and A. M. Kudo, Major-element variations of late Cenozoic basalts of New Mexico, *Spec. Publ. N. M. Geol. Soc.*, *5*, 82–88, 1976.

Bachman, G. O., and H. H. Mehnert, New K-Ar dates and the late Pliocene to Holocene geomorphic history of the central Rio Grande region, New Mexico, *Geol. Soc. Am. Bull.*, *89*, 283–292, 1978.

Baldridge, W. S., Petrology and petrogenesis of Plio-Pleistocene basaltic rocks from the central Rio Grande rift, New Mexico, and their relation to rift structure, in *Rio Grande Rift: Tectonics and Magmatism*, edited by R. E. Riecker, pp. 323–353, AGU, Washington, D. C., 1979.

Baldridge, W. S., F. V. Perry, and E. S. Gladney, Petrology and geochemistry of the Cat Hills volcanic field, central Rio Grande rift, New Mexico, *Geol. Soc. Am. Bull.*, 93, 635–643, 1982.

Baldridge, W. S., Y. Bartov, and A. Kron, Geologic map of the Rio Grande rift and Southeastern Colorado Plateau, New Mexico and Arizona, scale 1:500,000, AGU, Washington D. C., 1983.

Baldridge, W. S., K. H. Olsen, and J. F. Callender, Rio Grande rift: problems and perspectives, *N. M. Geol. Soc. Guideb.*, *35*, 1–12, 1984.

Baldridge, W. S., F. V. Perry, and M. Shafiqullah, Late Cenozoic volcanism of the southeastern Colorado Plateau I: Volanic geology of the Lucero area, New Mexico, *Geol. Soc. Am. Bull*, in press, 1987.

Basaltic Volcanism Study Project, *Basaltic Volcanism on the Terrestrial Planets*, 1286 pp., Pergamon, New York, 1981.

Batiza, R., Inverse relationship between Sr isotope diversity and rate of oceanic volcanism has implications for mantle heterogeneity, *Nature*, *309*, 440–441, 1984.

Brookins, D. G., and A. W. Laughlin, Rb-Sr geochronologic investigation of Precambrian samples from deep geothermal drill holes, Fenton Hill, New Mexico, *J. Volcanol. Geotherm. Res.*, *15*, 43–58, 1983.

Brookins, D. G., and A. Majumdar, The Sandia granite, New Mexico—Biotite metamorphic and whole rock Rb-Sr ages, *Isochron West*, *33*, 19–20, 1982.

Brookins, D. G., W. R. Bolton, and K. C. Condie, Rb-Sr isochron ages of four Precambrian igneous rock units from south-central New Mexico, *Isochron West*, *29*, 31–37, 1980.

Brookins, D. G., M. E. Balestri, and P. D. Fullagar, Rb-Sr data from miscellaneous Precambrian rocks, northern New Mexico, *Isochron West*, *42*, 10–11, 1985.

Buck, W. R., Small-scale convection induced by passive rifting: The cause for uplift of rift shoulders, *Earth Planet. Sci. Lett.*, *77*, 362–372, 1986.

Bultitude, R. J., and D. H. Green, Experimental study of crystal-liquid relationships at high pressures in olivine nephelinite and basanite compositions, *J. Petrol.*, *12*, 121–147, 1971.

Carlson, R. W., Isotopic constraints on Columbia River flood basalt genesis and the nature of the subcontinental mantle, *Geochim. Cosmochim., Acta*, *48*, 2357–2372, 1984.

Chapin, C. E., Evolution of the Rio Grande rift—A summary, in *Rio Grande Rift: Tectonics and Magmatism*, edited by R. E. Riecker, pp. 1–5, AGU, Washington, D. C., 1979.

Cordell, L., Regional geophysical setting of the Rio Grande rift, *Geol. Soc. Am. Bull.*, *89*, 1073–1090, 1978.

Cordell, L., Extension in the Rio Grande rift, *J. Geophys. Res.*, *87*, 8561–8569, 1982.

Crowley, J. C., Strontium isotope and rare earth element analysis of Rio Grande rift basalts: Implications for magmagenesis in continental rifts, Ph.D. dissertation, 116 pp., Brown Univ., Providence, R. I., 1984.

Daggett, P., G. R. Keller, and P. Morgan, Crustal structure studies in the southern Rio Grande rift, *Earthquake Notes, 52*, 53, 1981.

Davies, G. F., Earth's neodymium budget and the structure and evolution of the mantle, *Nature, 290*, 208–213, 1981.

Davies, G. F., Geophysical and isotopic constraints on mantle convection: An interim synthesis, *J. Geophys. Res., 89*, 6017–6040, 1984.

DePaolo, D. J., Estimation of the depth of origin of basic magmas: A modified thermodynamic approach and a comparison with experimental melting studies, *Contrib. Mineral. Petrol., 69*, 265–278, 1979.

DePaolo, D. J., A neodymium and strontium isotopic study of the Mesozoic calk-alkaline granitic batholiths of the Sierra Nevada and Peninsular ranges, California, *J. Geophys. Res., 86*, 10,470–10,488, 1981*a*.

DePaolo, D. J., Nd in the Colorado Front Range and implications for crust formation and mantle evolution in the Proterozoic, *Nature, 291*, 193–196, 1981*b*.

DePaolo, D. J., Trace element and isotopic effects of combined wallrock assimilation and fractional crystallization, *Earth Planet. Sci. Lett., 53*, 189–202, 1981*c*.

DePaolo, D. J., Isotopic studies of processes in mafic magma chambers, I, The Kiglapait intrusion, Labrador, *J. Petrol., 26*, 925–951, 1985.

DePaolo, D. J., and G. J. Wasserburg, Inferences about magma sources and mantle structure from variations of $^{143}Nd/^{144}Nd$, *Geophys. Res. Lett., 3*, 743–746, 1976*a*.

DePaolo, D. J., and G. J. Wasserburg, Nd isotopic variations and petrogenetic models, *Geophys. Res. Lett., 3*, 249–252, 1976*b*.

DePaolo, D. J., and G. J. Wasserburg, The sources of island arcs as indicated by Nd and Sr isotopic studies, *Geophys. Res. Lett., 4*, 465–468, 1977.

DePaolo, D. J., and G. J. Wasserburg, Neodymium isotopes in flood basalts from the Siberian Platform and inferences about their mantle sources, *Proc. Natl. Acad. Sci. U. S. A., 76*, 3056–3060, 1979*a*.

DePaolo, D. J., and G. J. Wasserburg, Petrogenetic mixing models and Nd-Sr isotopic patterns, *Geochim. Cosmochim. Acta, 43*, 615–627, 1979*b*.

DePaolo, D. J., W. I. Manton, E. S. Grew, and M. Halpern, Sm-Nd, Rb-Sr, and U-Th-Pb systematics of granulite facies rocks from Fyfe Hills, Enderby Land, Antarctica, *Nature, 298*, 614–618, 1982.

Drake, M. J., and D. F. Weill, Partition of Sr, Ba, Ca, Y, Eu^{2+}, Eu^{3+}, and other REE between plagioclase feldspar and magmatic liquid: An experimental study, *Geochim. Cosmochim. Acta, 39*, 689–712, 1975.

Dungan, M. A., R. L. Nielsen, and D. Phelps, Spatial and temporal variation patterns in late Cenozoic basaltic volcanism, NE Jemez lineament, northern New Mexico, *Geol. Soc. Am. Abstr. Programs, 15*, 379, 1983.

Dungan, M. A., W. R. Muehlberger, L. Leininger, C. Peterson, N. J. McMillan, G. Gunn, M. Lindstrom, and L. Haskin, Volcanic and sedimentary stratigraphy of the Rio Grande gorge and late Cenozoic evolution of the southern San Luis Valley, *Field Conf. Guideb. N.M. Geol. Soc., 35*, 157–170, 1984.

Dungan, M. A., M. M. Lindstrom, N. J. McMillan, S. Moorbath, J. Hoefs, and L. A. Haskin, Open system magmatic evolution of the Taos Plateau volcanic field, northern New Mexico, 1, The petrology and geochemistry of the Servilleta basalt, *J. Geophys. Res., 91*, 5999–6028, 1986.

Dupré, B., and C. J. Allègre, Pb-Sr isotope variation in Indian Ocean basalts and mixing phenomena, *Nature, 303*, 142–146, 1983.

Dupuy, C., and J. Dostal, Trace element geochemistry of some continental tholeiites, *Earth Planet. Sci. Lett., 67*, 61–69, 1984.

Farmer, G. L., Isotope geochemistry of Mesozoic and Tertiary igneous rocks in the western U.S. and implication for the structure and composition of the deep continental lithosphere, in *Metamorphic and Crustal Evolution of the Western United States*, Rubey vol. VII, edited by W. G. Ernst, Prentice-Hall, Englewood Cliffs, N. J., in press, 1987.

Farmer, G. L., and D. J. DePaolo, Origin of Mesozoic and Tertiary granite in the western United States and implications for pre-Mesozoic crustal structure, 1, Nd and Sr isotopic studies in the geocline of the northern Great Basin, *J. Geophys. Res., 88*, 3379–3401, 1983.

Fitton, J. G., and H. M. Dunlop, The Cameroon line, West Africa, and its bearing on the origin of oceanic and continental alkali basalt, *Earth Planet. Sci. Lett., 72*, 23–38, 1985.

Fraser, K. J., C. J. Hawksworth, A. J. Erlank, R. H. Mitchell, and B. H. Scott-Smith, Sr, Nd, and Pb isotope and minor element geochemistry of lamproites and kimberlites, *Earth Planet. Sci. Lett., 76*, 57–70, 1986.

Frey, F. A., D. H. Green, and S. D. Roy, Integrated models of basalt petrogenesis: A study of quartz tholeiites to olivine melilitites from southeastern Australia utilizing geochemical and experimental petrological data, *J. Petrol., 19*, 463–513, 1978.

Fujii, T., and H. Bougault, Melting relations of a magnesian abyssal tholeiite and the origin of MORBs, *Earth Planet. Sci. Lett., 62*, 283–295, 1983.

Gill, J. B., Sr-Pb-Nd isotopic evidence that both MORB and OIB sources contribute to oceanic island arc magmas in Fiji, *Earth Planet. Sci. Lett., 68*, 443–458, 1984.

Gish, D. M., G. R. Keller, and M. L. Sbar, A refraction study of deep crustal structure in the Basin and Range: Colorado Plateau of eastern Arizona, *J. Geophys. Res, 86*, 6029–6038, 1981.

Green, D. H., A review of experimental evidence on the origin of basaltic and nephelinitic magmas, *Phys. Earth Planet. Inter., 3*, 221–235, 1970.

Green, D. H., Composition of basaltic magmas as indicators of conditions of origin: Application to oceanic volcanism, *Philos. Trans. R. Soc. London, Ser. A, 268*, 707–725, 1971.

Hanson, G. N., Rare earth elements in petrogenetic studies of igneous sytems, *Annu. Rev. Earth Planet. Sci., 8*, 371–406, 1980.

Hart, S. R., A large-scale isotope anomaly in the southern hemisphere mantle, *Nature, 309*, 753–757, 1984.

Hart, W. K., Chemical and isotopic evidence for mixing between depleted and enriched mantle, northwestern U.S.A., *Geochim. Cosmochim. Acta, 49*, 131–144, 1985.

Hofmann, A. W., and W. M. White, Mantle plumes from ancient oceanic crust, *Earth Planet. Sci. Lett., 57*, 421–436, 1982.

Irvine, T. N., and W. R. A. Baragar, A guide to the chemical classification of the common volcanic rocks, *Can. J. Earth Sci., 8*, 523–548, 1971.

Jagoutz, E., R. W. Carlson, and G. W. Lugmair, Equilibrated Nd-unequilibrated Sr isotopes in mantle xenoliths, *Nature, 286*, 708–710, 1980.

Jaques, A. L., and D. H. Green, Anhydrous melting of peridotite at 0-15 Kb pressure and the genesis of tholeiitic basalts, *Contrib. Mineral. Petrol., 73*, 287–310, 1980.

Keller, G. R., L. W. Braile, and P. Morgan, Crustal structure, geophysical models and contemporary tectonism of the Colorado Plateau, *Tectonophysics, 61*, 131–147, 1979*a*.

Keller, G. R., L. W. Braile, and J. W. Schlue, Regional crustal structure of the Rio Grande rift from surface wave dispersion measurements, in *Rio Grande Rift: Tectonics and Magmatism*, edited by R. E. Riecker, pp. 115–126, AGU, Washington D. C., 1979*b*.

Kudo, A. M., V. C. Kelly, P. E. Damon, and M. Shafiqullah, K-Ar ages of basalt flows at Canjilon Hill, Isleta Volcano, and Cat Hills volcanic field, Albuquerque-Belen basin, central New Mexico, *Isochron West, 18*, 15–16, 1977.

Kushiro, I., Compositions of magmas formed by partial zone melting of the earth's upper mantle, *J. Geophys. Res, 73*, 619–634, 1968.

Kushiro, I., Density of tholeiite and alkali basalt magmas at high pressures, *Year Book Carnegie Inst. Washington, 81*, 305–309, 1982.

Laughlin, A. W., D. G. Brookins, and J. D. Causey, Late Cenozoic basalts from the Bandera lava field, Valencia County, New Mexico, *Geol. Soc. Am. Bull., 83*, 1543–1551, 1972.

Laughlin, A. W., D. G. Brookins, and P. E. Damon, Late Cenozoic basaltic volcanism along the Jemez zone of New Mexico and Arizona, *Geol. Soc. Am. Abstr. Programs, 8*, 598, 1976.

Laughlin, A. W., D. G. Brookins, P. E. Damon, and M. Shafiqullah, Late Cenozic volcanism of the central Jemez zone, Arizona-New Mexico, *Isochron West, 25*, 5–8, 1979.

Laughlin, A. W., M. J. Aldrich, Jr., M. E. Ander, G. H. Heiken, and D. T. Vaniman, Tectonic setting and history of late Cenozoic volcanism in west-central New Mexico, *Field Conf. Guideb. N. M. Geol. Soc., 33*, 279–284, 1982.

Lipman, P. W., Alkalic and tholeiitic basaltic volcanism related to the Rio Grande depression, southern Colorado and northern New Mexico, *Geol. Soc. Am. Bull., 80*, 1343–1354, 1969.

Lipman, P. W., and H. H. Mehnert, Late Cenozoic basaltic volcanism and development of the Rio Grande depresssion in the southern Rocky Mountains, *Mem. Geol. Soc. Am., 144*, 119–154, 1975.

Lipman, P. W., and H. H. Mehnert, The Taos Plateau volcanic field, northern Rio Grande rift, New Mexico, in *Rio Grande Rift: Tec-*

tonics and Magmatism, edited by R. E. Riecker pp. 289–311, AGU, Washington, D. C., 1979*a*.

Lipman, P. W., and H. H. Mehnert, Potassium-argon ages from the Mount Taylor volcanic field, New Mexico, *U.S. Geol. Surv. Prof. Pap., 1124-B*, 8 pp., 1979*b*.

Lipman, P. W., and R. H. Moench, Basalts of the Mount Taylor volcanic field, New Mexico, *Geol. Soc. Am. Bull., 83*, 1335–1344, 1972.

Loeffler, B. M., and K. Futa, Sr and Nd isotope systematics of the Jemez volcanic field, *Eos Trans. AGU, 66*, 1110, 1985.

Luedke, R. G., and R. L. Smith, Map showing distribution, composition, and age of late Cenozoic volcanic centers in Arizona and New Mexico, scale 1:1,000,000, *U.S. Geol. Surv. Misc. Invest. Ser., Map I-1091-A*, 1978.

Mayo, E. B., Lineament tectonics and some ore districts of the southwest, *Trans. Am. Inst. Min. Metall. Pet. Eng., 211*, 1169–1175, 1958.

McKenzie, D., and R. K. O'Nions, Mantle reservoirs and ocean island basalts, *Nature, 301*, 229–231, 1983.

Menzies, M. A., W. P. Leeman, and C. J. Hawksworth, Isotope geochemistry of Cenozoic volcanic rocks reveals mantle heterogeneity below western USA, *Nature, 303*, 205–209, 1983.

Menzies, M. A., P. Kempton, and M. Dungan, Interaction of continental lithosphere and asthenospheric melts below the Geronimo volcanic field, Arizona, U.S.A., *J. Petrol., 26*, 663–693, 1985.

Moretti, I., and C. Froidevaux, Thermomechanical models of active rifting, *Tectonics, 5*, 501–511, 1986.

Morris, J. D., and S. R. Hart, Isotopic and incompatible element constraints on the genesis of island arc volcanics from Cold Bay and Amak Island, Aleutians, and implications for mantle structure, *Geochim. Cosmochim. Acta, 47*, 2015–2030, 1983.

Mukhopadhyay, B., D. G. Brookins, and S. L. Bolivar, Rb-Sr wholerock study of the Precambrian rocks of the Pedernal Hills, New Mexico, *Earth Planet. Sci. Lett., 27*, 283–286, 1975.

Nelson, B. K., and D. J. DePaolo, Rapid production of continental crust 1.7 to 1.9 b.y. ago: Nd isotopic evidence from the basement of the North American midcontinent, *Geol. Soc. Am. Bull., 96*, 746–754, 1985.

Nicholls, J., I. S. E. Carmichael, and J. C. Stormer, Jr., Silica activity and P_{total} in igneous rocks, *Contrib. Mineral. Petrol., 33*, 1–20, 1971.

Nichols, R. L., McCartys basalt flow, Valencia Country, New Mexico, *Geol. Soc. Am. Bull., 57*, 1049–1086, 1946.

Nielsen, R. L., EQUIL: A program for the modeling of low-pressure differentiation processes in natural mafic magma bodies, *Comput. Geosci., 11*, 531–546, 1985.

Nielsen, R. L., and M. A. Dungan, Low pressure mineral-melt equilibria in natural anhydrous mafic systems, *Contrib. Mineral. Petrol., 84*, 310–326, 1983.

Olsen, K. H., G. R. Keller, and J. N. Stewart, Crustal structure along the Rio Grande rift from seismic refraction profiles, in *Rio Grande Rift: Tectonics and Magmatism*, edited by R. E. Riecker, pp. 127–143, AGU, Washington, D. C., 1979.

Olsen, K. H., W. S. Baldridge, and J. F. Callender, Rio Grande rift: An overview, *Tectonophysics*, in press, 1987.

Perry, F. V., D. J. DePaolo, and W. S. Baldridge, Nd and Sr evidence for the origin of Mount Taylor lavas and depleted mantle beneath the Colorado Plateau-Rio Grande rift, central New Mexico, *Eos Trans. AGU, 64*, 753, 1983.

Phelps, D. W., D. A. Gust, and J. L. Wooden, Petrogenesis of the mafic feldspathoidal lavas of the Raton-Clayton volcanic field, New Mexico, *Contrib. Mineral. Petrol., 84*, 182–190, 1983.

Presnall, D. C., and J. D. Hoover, Composition and depth of origin of primary mid-ocean ridge basalts, *Contrib. Mineral. Petrol., 87*, 170–178, 1984.

Presnall, D. C., S. A. Dixon, J. R. Dixon, T. H. O'Donnell, N. L. Brenner, R. L. Schrock, and D. W. Dycus, Liquidus phase relations on the join diopside-forsterite-anorthite from 1 atm to 20 kbar: Their bearing on the generation and crystallization of basaltic magma, *Contrib. Mineral. Petrol., 66*, 203–220, 1978.

Presnall, D. C., J. R. Dixon, T. H. O'Donnell, and S. A. Dixon, Generation of mid-ocean ridge tholeiites, *J. Petrol., 20*, 3–35, 1979.

Rinehart, E. J., A. R. Sanford, and R. M. Ward, Geographic extent and shape of an extensive magma body at midcrustal depths in the Rio Grande rift near Socorro, New Mexico, in *Rio Grande Rift: Tectonics and Magmatism*, edited by R. E. Riecker, pp. 237–251, AGU, Washington, D. C., 1979.

Roller, J. C., Crustal structure in the eastern Colorado Plateau province from seismic refraction measurements, *Bull. Seismol. Soc. Am., 55*, 107–119, 1965.

Rudnick R. L., S. M. McLennan, and S. R. Taylor, Large ion lithophile elements in rocks from high-pressure granulite facies terrains, *Geochim. Cosmochim. Acta, 49*, 1645–1655, 1985.

Seager, W. R., M. Shafiqullah, J. W. Hawley, and R. F. Marvin, New K-Ar dates from basalts and the evolution of the southern Rio Grande rift, *Geol. Soc. Am. Bull., 95*, 87–99, 1984.

Sinno, Y. A., P. H. Dagget, G. R. Keller, P. Morgan, and S. H. Harder, Crustal structure of the southern Rio Grande rift determined from seismic refraction profiling, *J. Geophys. Res., 91*, 6143–6156, 1986.

Smith, R. L., and R. G. Luedke, Potentially active volcanic lineaments and loci in western conterminous United States, in *Explosive Volcanism: Inception, Evolution, and Hazards*, pp. 47–66, National Academy Press, Washington, D. C., 1984.

Spera, F. J., Carbon dioxide in petrogenesis, III, Role of volatiles in the ascent of alkaline magma with special reference to xenolith-bearing lavas, *Contrib. Mineral. Petrol., 88*, 217–232, 1984.

Spohn, T., and G. Schubert, Convective thinning of the lithosphere: A mechanism for rifting and mid-plate volcanism on Earth, Venus, and Mars, *Tectonophysics, 94*, 67–90, 1983.

Stewart, W. E., and L. C. Pakiser, Crustal structure in eastern New Mexico interpreted from the Gnome explosion, *Bull. Seismol. Soc. Am., 52*, 1017–1030, 1962.

Stormer, J. C., Jr., Mineralogy and petrology of the Raton-Clayton volcanic field, northeastern New Mexico, *Geol. Soc. Am. Bull., 83*, 3299–3322, 1972.

Sun, S. S., R. W. Nesbitt, and A. Sharaskin, Geochemical characteristics of mid-ocean ridge basalts, *Earth Planet. Sci. Lett., 44*, 119–138, 1979.

Taggart, J. E., and D. G. Brookins, Rb-Sr whole rock age determinations for Sandia granite and Cibola gneiss, New Mexico, *Isochron West, 12*, 5–8, 1975.

Takahashi, E., Melting relations of an alkali-olivine basalt to 30 kbar, and their bearing on the origin of alkali basalt magmas, *Year Book Carnegie Inst. Washington, 79*, 271–276, 1980.

Takahashi, E., and I. Kushiro, Melting of dry peridotite at high pressures and basalt magma genesis, *Am. Mineral., 68*, 859–879, 1983.

Thompson, G. A., and M. L. Zoback, Regional geophysics of the Colorado Plateau, *Tectonophysics, 61*, 149–181, 1979.

Thompson, R. N., A. P. Dicken, I. L. Gibson, and M. A. Morrison, Elemental fingerprints of isotopic contamination of Hebridean Palaeocene mantle-derived magmas by Archean sial, *Contrib. Mineral. Petrol., 79*, 159–168, 1982.

Toppozada, T. R., and A. R. Sanford, Crustal structure in central New Mexico interpreted from the Gasbuggy explosion, *Bull. Seismol. Soc. Am., 66*, 877–886, 1976.

Vaniman, D., A. W. Laughlin, and E. S. Gladney, Navajo minettes in the Cerros de las Mujeres, New Mexico, *Earth Planet. Sci. Lett., 74*, 69–80, 1985.

Van Schmus, W. R., and M. E. Bickford, Proterozoic chronology and evolution of the mid-continent region: North America, in *Precambrian Plate Tectonics*, edited by A. Kroner, pp. 261–296, Elsevier, New York, 1981.

Vollmer, R., P. Ogden, J.-G. Schilling, R. H. Kingsley, and D. G. Waggoner, Nd and Sr isotopes in ultrapotassic volcanic rocks from the Leucite Hills, Wyoming, *Contrib. Mineral. Petrol., 87*, 359–368, 1984.

Warren, D. H., A seismic refraction survey of crustal structure in central Arizona, *Geol. Soc. Am. Bull., 80*, 257–282, 1969.

White, D. L., Rb-Sr isochron ages of some Precambrian plutons in south-central New Mexico, *Isochron West, 21*, 8–14, 1978.

White, W. M., Sources of oceanic basalts: Radiogenic isotopic evidence, *Geology, 13*, 115–118, 1985.

Williams, S., Oceanic mantle beneath the Rio Grande rift: Isotopic and trace element evidence of crustal contamination of mantle-derived melts, *Eos Trans. AGU, 64*, 338, 1983.

Williams, S., Late Cenozoic volcanism in the Rio Grande rift: Trace element, strontium, and neodymium isotopic geochemistry of the Taos Plateau volcanic field, Ph.D. dissertation, 239 pp., Univ. of Minn., Minneapolis, 1984.

Wilshire, H. G., Mantle metasomatism: The REE story, *Geology , 12*, 395–398, 1984.

Wobus, R. A., and C. E. Hedge, Rb-Sr isochron age of Precambrian plutons of the San Pedro mountains, north-central New Mexico, *Isochron West, 27*, 19–25, 1980.

Yoder, H. S., and C. E. Tilley, Origin of basaltic magmas: an experimental study of natural and synthetic rock systems, *J. Petrol., 3*, 342–532, 1962.

Zartman, R. E., and B. R. Doe, Plumbotectonics-the model, *Tectonophysics*, *75*, 135–162, 1981.

Zindler, A., Geochemical processes in the earth's mantle and nature of crust-mantle interactions: evidence from studies of neodymium and strontium isotope ratios in mantle-derived igneous rocks and lherzolite nodules, Ph.D. dissertation, Mass. Inst. of Technol., Cambridge, 1980.

Zindler, A., and S. Hart, Chemical geodynamics, *Annu. Rev. Earth Planet. Sci.*, *14*, 493–571, 1986.

Zindler, A., and E. Jagoutz, Mantle cryptology, *Geochim. Cosmochim. Acta*, in press, 1987.

Zindler, A., H. Staudigel, and R. Batiza, Isotope and trace element geochemistry of young Pacific seamounts: Implications for the scale of upper mantle heterogeneity, *Earth Planet. Sci. Lett.*, *70*, 175–195, 1984.

Zoback, M. L., and M. Zoback, State of stress in the conterminous United States, *J. Geophys. Res.*, *85*, 6113–6156, 1980.

W. S. Baldridge, Earth and Space Sciences Division, MS-D462, Los Alamos National Laboratory, Los Alamos, NM 87545.

D. J. DePaolo, Department of Earth and Space Sciences, University of California, Los Angeles, CA 90024.

F. V. Perry, Isotope and Nuclear Chemistry Division, MS-J514, Los Alamos National Laboratory, Los Alamos, NM 87545.

(Received October 9, 1986;
revised April 23, 1987;
accepted April 30, 1987.)